

AD-A069 301

AIR FORCE INST OF TECH WRIGHT-PATTERSON AFB OHIO SCH--ETC F/G 1/3  
INVESTIGATION OF ROLL PERFORMANCE FOR A HIGHLY NONLINEAR STATIC--ETC(U)  
MAR 79 P L VERGEZ

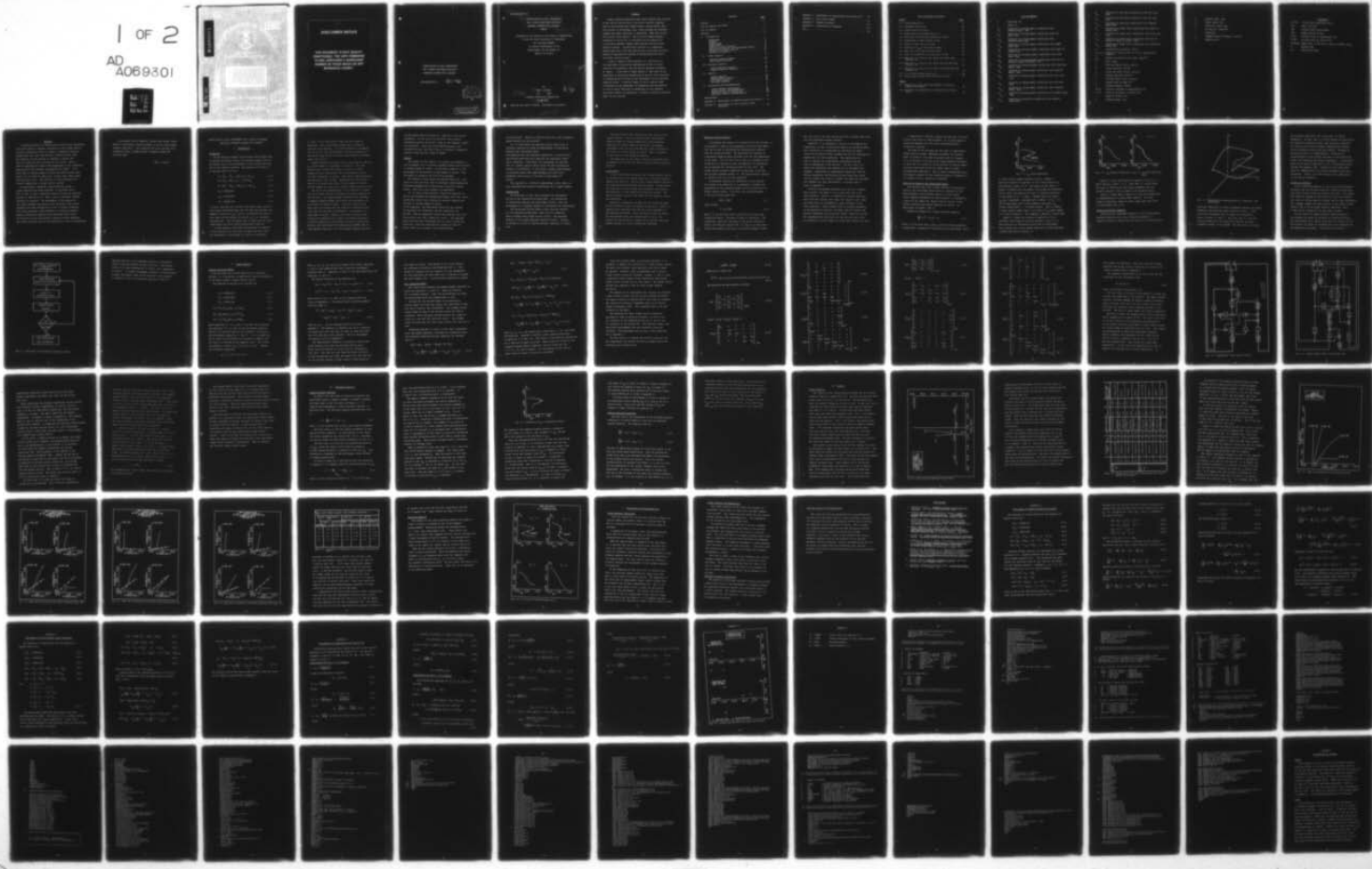
UNCLASSIFIED

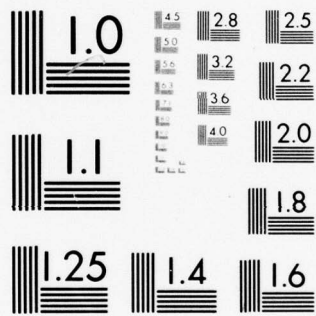
AFIT/G6C/EE/79-4

NL

1 OF 2

AD  
A069301





MICROCOPY RESOLUTION TEST CHART  
NATIONAL BUREAU OF STANDARDS-1963-A

## **DISCLAIMER NOTICE**

**THIS DOCUMENT IS BEST QUALITY  
PRACTICABLE. THE COPY FURNISHED  
TO DDC CONTAINED A SIGNIFICANT  
NUMBER OF PAGES WHICH DO NOT  
REPRODUCE LEGIBLY.**

INVESTIGATION OF ROLL PERFORMANCE  
FOR A HIGHLY NONLINEAR STATICALLY  
UNSTABLE FIGHTER-TYPE AIRCRAFT

AFIT/GGC/EE/79-4

Paul L. Vergez  
2nd Lt USAF

DDC  
RECEIVED  
JUN 4 1979  
A

DISTRIBUTION STATEMENT A

Approved for public release  
Distribution Unlimited

79 05 00 238

14

AFIT/GGC/EE/79-4

INVESTIGATION OF ROLL PERFORMANCE  
FOR A HIGHLY NONLINEAR STATICALLY  
UNSTABLE FIGHTER-TYPE AIRCRAFT.

THESIS

9) Master's thesis,

Presented to the Faculty of the School of Engineering  
of the Air Force Institute of Technology  
Air Training Command  
in Partial Fulfillment of the  
Requirements for the Degree of  
Master of Science

Accession For	
NTIS GRA&I	<input checked="" type="checkbox"/>
ROC TAB	<input type="checkbox"/>
Unannounced	<input type="checkbox"/>
Justification	
By	
Distribution/	
Availability Codes	
Dist	Avail and/or special
A	23 off

12) LCP/1p.

10) by Paul L. Vergez  
2Lt USAF

Graduate Electrical Engineering

11) March 1979

Approved for public release; distribution unlimited

012 225

LB

## Preface

A major problem confronting some modern fighter-type aircraft is the loss of control due to roll-pitch inertial coupling. Some of the aircraft have flight control systems which, when the aircraft is performing a roll, sense pitchup and therefore command nose down stabilator to saturation. When this occurs the aircraft loses control. The Air Force Flight Dynamics Laboratory at W.P.A.F.B. is interested in the analysis of a statically unstable fighter-type aircraft flying at high angles of attack. Of particular interest is a comparison between body axis rolls and velocity axis rolls and a possible method of analyzing the problem of uncontrollability due to the flight control system.

I wish to thank my thesis advisor, Dr. John D'Azzo of the Department of Electrical Engineering of the Air Force Institute of Technology, for his overall guidance throughout my thesis. I also wish to thank Captain J. Gary Reid of the Department of Electrical Engineering of the Air Force Institute of Technology for his help in the development of the nonlinear equation solver. A special thanks is due to Captain James Silverthorn of the Department of Aeronautics and Astronautics of the Air Force Institute of Technology for his patience and timely efforts in helping me to develop a working linearized model of the aircraft.

## Contents

	<u>Page</u>
Preface . . . . .	ii
List of Figures and Tables . . . . .	v
List of Symbols . . . . .	vi
Abstract . . . . .	xi
I. Introduction . . . . .	1
Background . . . . .	1
Purpose . . . . .	3
Organization . . . . .	4
Linear Model . . . . .	5
Method of Linear Analysis . . . . .	6
Bifurcation Analysis and Catastrophe Theory . . . . .	8
Method of Nonlinear Analysis . . . . .	10
Validity of Analysis . . . . .	12
II. Linear Analysis . . . . .	15
Reduced Linearized Model . . . . .	15
Full Linearized Model . . . . .	17
III. Nonlinear Analysis . . . . .	30
Single Nonlinear Equation . . . . .	30
Coupled Nonlinear Equations . . . . .	33
IV. Results . . . . .	35
Linear Analysis . . . . .	35
Reduced Model Analysis . . . . .	35
Full Model Analysis . . . . .	37
Nonlinear Analysis . . . . .	45
V. Conclusions and Recommendations . . . . .	47
Linear Analysis Conclusions . . . . .	47
Linear Analysis Recommendations . . . . .	48
Nonlinear Analysis Conclusions . . . . .	48
Nonlinear Analysis Recommendations . . . . .	49
Bibliography . . . . .	50
Appendix A: Development of Reduced Linearized Equation . . . . .	51
Appendix B: Development of Full Aircraft Linear Equations . . . . .	55

Appendix C: Development of Longitudinal and Lateral FCS . .	58
Appendix D: Root Locus Example . . . . .	62
Appendix E: Computer Programs . . . . .	63
Appendix F: Explanations of Programs . . . . .	82
Vita . . . . .	85

List of Figures and Tables

<u>Figure</u>	<u>Page</u>
1.1 X With Bifurcation . . . . .	9
1.2 X Without Bifurcation . . . . .	10
1.3 X With Inflection Point . . . . .	10
1.4 Characteristic Representation of X . . . . .	11
1.5 Flow Chart for Nonlinear Equation(s) Solver . . . . .	13
2.1 Longitudinal Flight Control System . . . . .	25
2.2 Lateral Flight Control System . . . . .	26
3.1 Shifting of $X_{eq}$ at Bifurcation Point . . . . .	32
4.1 Root Locus For Reduced Linear Model . . . . .	36
4.2 Lines of Instability for Variations in AOA . . . . .	40
4.3 Body Axis vs. Velocity Axis Rolls with Dual Longitudinal FCS . . . . .	41
4.4 Body Axis vs. Velocity Axis Rolls with Low AOA Longitudinal FCS . . . . .	42
4.5 Body Axis vs. Velocity Axis Rolls with High AOA Longitudinal FCS . . . . .	43
4.6 X vs $C_2$ for Various Values of $C_1$ . . . . .	46
D.1 Closed Loop and Open Loop Roots for Aircraft . . . . .	62

Tables

4.1 Variations in AOA, With and Without the Aileron Rudder Interconnect . . . . .	38
4.2 Occurance of Instability for Aircraft with Various FCS's. . . . .	44

### List of Symbols

b	Wing span, ft.
c	Chord, ft.
$C_{L\beta}$	Variation of rolling moment coefficient with sideslip angle, /rad.
$C_{Lp}$	Variation of rolling moment coefficient with roll rate, /rad.
$C_{L\delta_f}$	Variation of rolling moment coefficient with flaperon angle, /deg.
$C_{L\delta_r}$	Variation of rolling moment coefficient with rudder angle, /deg.
$C_{M\alpha}$	Variation of pitching moment coefficient with angle of attack, /rad.
$C_{Mq}$	Variation of pitching moment coefficient with pitch rate, /rad.
$C_{M\dot{\alpha}}$	Variation of pitching moment coefficient with rate of change of angle of attack, /rad.
$C_{M\delta_s}$	Variation of pitching moment coefficient with stabilizer angle, /deg.
$C_{n\beta}$	Variation of yawing moment coefficient with sideslip angle, /rad.
$C_{np}$	Variation of yawing moment coefficient with roll rate, /rad.
$C_{nr}$	Variation of yawing moment coefficient with yaw rate, /rad.
$C_{n\delta_f}$	Variation of yawing moment coefficient with flaperon angle, /deg.
$C_{n\delta_r}$	Variation of yawing moment coefficient with rudder angle, /deg.
$C_{y\beta}$	Variation of side-force coefficient with sideslip angle, /rad.

$C_{Yp}$	Variation of side-force coefficient with roll rate, /rad.
$C_{Yr}$	Variation of side-force coefficient with yaw rate, /rad.
$C_{Y\delta_f}$	Variation of side-force coefficient with flaperon angle, /deg.
$C_{z\alpha}$	Variation of normal force coefficient with angle of attack, /rad.
$C_{zq}$	Variation of normal force coefficient with pitch rate, /rad.
$C_{z\dot{\alpha}}$	Variation of normal force coefficient with rate of change of angle of attack, /rad.
$C_{z\delta_s}$	Variation of normal force coefficient with stabilizer angle, /deg.
$g$	Acceleration of gravity, ft/sec.
$I_x, I_y, I_z$	Moments of inertia about X, Y, Z axis respectively, slug-ft <sup>2</sup> .
$J_{xz}$	Product of inertia in XZ plane, slug-ft <sup>2</sup> .
$m$	Mass, slugs.
$p$	Roll rate about X-axis, rad/sec.
$PC$	Static pressure, lbs/ft <sup>2</sup> .
$q$	Pitch rate about Y-axis, rad/sec.
$\bar{q}$	Dynamic pressure, lbs/ft <sup>2</sup> .
$r$	Yaw rate about Z-axis, rad/sec.
$s$	Surface area of wing, ft <sup>2</sup> .
$U$	Forward velocity, ft/sec.
X1-X5	Physical variables in longitudinal FCS.
Z1-Z4	Physical variables in lateral FCS.
$\alpha$	Angle of attack, rad.
$\beta$	Sideslip angle, rad.

$\delta_f$	Flaperon angle, deg.
$\delta_r$	Rudder angle, deg.
$\delta_s$	Stabilizer angle, deg.
$\rho$	Air density, slugs/ft <sup>3</sup> .
$\lambda$	Eigenvalue.
$\omega_n$	Undamped natural frequency, rad/sec.
$\zeta$	Damping ratio.

### Subscripts

$[A^{-1}B]$	An nxn plant coefficient matrix.
AOA	Angle of attack.
ARI	Aileron rudder interconnect.
FCS	Flight Control System
F3,F4	Variable gains in longitudinal FCS.
F7,F8	Variable gains in lateral FCS.
KF,KR,KS	Dummy gains in FCS used to analyze feedback loops.
P	Phugoid mode.
SP	Short period mode.

### Abstract

A linearized model of a fighter-type aircraft with significant roll-pitch inertial coupling, including its full flight control system, is required in order to conduct a comparative analysis between body axis rolls and velocity (stability) axis rolls. The stability of the aircraft is checked at various roll rates for both body axis and velocity axis rolls. This is done by examining the signs of the eigenvalues of the linearized model-positive for unstable and negative for stable. It is found that at various angles of attack the velocity axis rolls prove to be at least as stable and, in most cases, more stable than body axis rolls. The stability is also observable for various combinations of flight control systems.

In developing a nonlinear coupled equation solver, a single equation with known solutions is considered first. This is done to show a simplified version of what the nonlinear program is required to do. Next, a pair of nonlinear coupled equations is analyzed. The development of the program for the single equation case proves to be successful, but certain problems arise when working with a pair of coupled equations. This thesis provides a good foothold on a method of analysis known as Bifurcation Analysis and Catastrophe Theory which can be used to solve the nonlinear coupled aircraft equations. This thesis presents some of the problem which could be encountered.

I also would like to thank Mr. Michael Bise and Mr. David Bowser of the Control Criteria Branch of the Air Force Flight Dynamics Laboratory. They proposed this topic and were very cooperative when I needed special information about the aircraft model.

Paul L. Vergez

INVESTIGATION OF ROLL PERFORMANCE FOR A HIGHLY NONLINEAR  
STATICALLY UNSTABLE FIGHTER-TYPE AIRCRAFT

I. Introduction

Background

As the design of fighter-type aircraft moves toward that of smaller and thinner wings, the nonlinear aspects play an increasing role in the performance of the aircraft and thus add to the stability problem. The equations of motion of an aircraft (Ref 1:11) are

$$\Sigma L = \dot{P}I_x - \dot{R}J_{xz} + QR(I_z - I_y) - PQ J_{xz} \quad (1.1)$$

$$\Sigma M = \dot{Q}I_y + PR(I_x - I_z) + (P^2 - R^2)J_{xz} \quad (1.2)$$

$$\Sigma N = \dot{R}I_z - \dot{P}J_{xz} + PQ(I_y - I_x) + QR J_{xz} \quad (1.3)$$

$$\Sigma F_x = m(\dot{U} + WQ - VR) \quad (1.4)$$

$$\Sigma F_y = m(\dot{V} + UR - WP) \quad (1.5)$$

$$\Sigma F_z = m(\dot{W} + VP - UQ) \quad (1.6)$$

It can be seen that for aircraft with larger wings, giving a more evenly distributed mass over the wing and fuselage, the moments of inertia ( $I_x$ ,  $I_y$ , and  $I_z$ ) are essentially equal to each other and the product of inertia ( $J_{xz}$ ) is considered insignificant. This de-couples the six equations into three longitudinal and three lateral-directional equations.

In some fighters, the weight distribution is primarily in the fuselage since the wings are small and thin, thus, the differences in the moments of inertia in equations

1.1 thru 1.3 are sufficiently large and they cannot be neglected. These differences produce what is known as inertial cross-coupling. If a rolling moment is introduced this results in some yawing moment, and the term  $PR(I_x - I_z)$  may become large enough to cause an uncontrollable pitching moment (Ref 1:183).

Another important coupling term is the product of inertia,  $J_{xz}$ , which appears in equations 1.1 thru 1.3. For some fighter-type aircraft the product of inertia is large enough to play a significant role in the analysis of the aircraft's equations of motion. This adds to the nonlinearity and coupling of the aircraft. Therefore, the task in this thesis is to analyze the effect of the product of inertia and all moments of inertia for a modern fighter-type aircraft.

Due to all the nonlinearities in the aircraft, it would also be of major interest to perform a nonlinear analysis of the aircraft. The Flight Dynamics Laboratory has developed a computer program (TIMEH) which gives the time history of an aircraft for desired inputs. The time histories have been useful in showing that the problem of instability does exist when the aircraft is performing a roll maneuver at a high angle of attack; however, the time histories do not provide any information as to where the problem originates. A possible approach to this problem is known as Bifurcation Analysis and Catastrophe Theory Methodology (BACTM) (Ref 4). This approach considers a set of nonlinear coupled equations

and determines their solutions as a function of the control parameters. In the case of an aircraft, these control parameters would be the pilot's input to the flaperon, rudder, and stabilator. Since the actual BACTM program is not available for use, the first step is to develop a comparable program, using the basic ideas of BACTM.

### Purpose

The purpose of this thesis is to analyze the problem of roll divergence for a statically unstable fighter-type aircraft at various angles of attack. Of particular interest is the performance of the aircraft at high angles of attack. This divergence is caused by the roll pitch coupling.

The problem is quite large and requires much work. This thesis is only the first step to eventually understanding the nonlinear phenomena and to then devise corrective control action. This first step contains two approaches:

(1) To look at the aircraft's linearized equations of motion and determine the maximum sustainable roll rate, before instability occurs, for a statically unstable fighter-type aircraft at various angles of attack.

In this approach the equilibrium conditions are assumed, the equations are linearized, and the eigenvalues are derived. When an eigenvalue crosses the imaginary axis into the positive real side, instability occurs. This approach gives some very good information but is rather limited and localized. Since the equations are linearized from the start, there is no insight to the nonlinearities

of the aircraft. There is a definite need for a more systematic global analysis of the aircraft.

(2) To investigate the nonlinear events which occur in nonlinear equations by using the methodology of bifurcation analysis and catastrophe theory.

This approach uses the nonlinear equation(s) to solve for the equilibrium conditions and linearizes the equation(s) about those conditions. From there, the eigenvalues are derived. This is a global analysis which allows the whole bifurcation surface to be obtained. It also gives a deeper understanding of nonlinear events like jump phenomena and limit cycle phenomena, which occurs in aircraft at high angles of attack.

This approach is a difficult undertaking so this thesis is only concerned with using the methodology for a simple example.

### Organization

The first part of this thesis presents the development and use of the linearized aircraft model. An introduction to bifurcation analysis and catastrophe follows; then the development of a computer program to incorporate this methodology.

The second part of this thesis starts with the analysis for the reduced aircraft model, then the full linearized model including full flight control system. The nonlinear analysis of the single nonlinear equation follows. Finally, an attempt at a pair of coupled nonlinear equations is looked into.

The third part of this thesis gives the results of the linear analysis: Effect of aileron-rudder interconnect, affect of angle of attack, comparison to specifications, comparison of reduced model to full model, and maximum sustainable roll rate for both body axis rolls and velocity axis rolls at various angles of attack. This is followed by the results of the nonlinear analysis.

The final part of this thesis gives the conclusions and recommendations for both the linear analysis and the nonlinear analysis.

#### Linear Model

A set of stability derivatives and a flight control system is selected from a wind tunnel model of a statically unstable fighter-type aircraft. The Air Force Flight Dynamics Laboratory has prepared time history data for this model. At high angles of attack the aircraft becomes uncontrollable, thus proving the usefulness of the stability derivatives and FCS. The control surfaces used for this model are the flaperon, rudder, and stabilator.

Some basic assumptions are made for the linearized model of the aircraft in order to simplify the analysis: Gravity is ignored which eliminates the sine and cosine dependence of the equations of motion. Since the perturbations are small, the second-order terms are assumed equal to zero. The velocity of the aircraft is assumed to be constant since the primary interest is in the steady-state solutions.

## Method of Linear Analysis

To determine the stability or instability of the aircraft, it is necessary to observe the eigenvalues of the aircraft model. This can be done by developing the characteristic equation from the linearized model. The characteristic equation is a polynomial equation whose factored roots are the eigenvalues of the model. The roll rate (P) is left as a variable in the characteristic equation so that the migration of eigenvalues can be observed for increasing values of roll rate. The flight control system is neglected in this part to see how the aircraft performs without it. The characteristic equation is limited to one set of trim conditions.

To determine stability or instability of the aircraft for various trim conditions it is necessary to observe the eigenvalues of the linearized model of the aircraft with its flight control system. To do this, the linearized model is set up in state space form

$$[A]\dot{X} = [B]X \quad (1.7)$$

which becomes

$$\dot{X} = [A^{-1}B]X \quad (1.8)$$

where X is an nx1 state vector and  $[A^{-1}B]$  is an nxn plant coefficient matrix. The matrix A must be invertible. The eigenvalues, which are the roots of the plant coefficient matrix, are obtained from  $[A^{-1}B]$ . As long as all the eigenvalues have negative real parts the aircraft remains stable,

but, once any of the roots become positive, the mode associated with the eigenvalue becomes unstable.

Therefore, it is important to be able to distinguish the eigenvalues in order to know which mode(s) can become unstable. This distinction is accomplished by obtaining the eigenvalues for the model without feedback and also by obtaining the eigenvectors for each eigenvalue. The eigenvectors are used to separate the longitudinal eigenvalues from the lateral eigenvalues of the aircraft. The next step is to obtain the eigenvalues and eigenvectors of the model with feedback. Separating the longitudinal eigenvalues from the lateral eigenvalues and plotting the open-loop roots along with the closed-loop roots on a graph, the modes for the model with feedback are then identifiable. A typical plot is shown in Appendix D.

To obtain the maximum sustained roll rate for a fighter-type aircraft, the model is set up with roll rate as an input variable. Since it is important to observe both body axis rolls and velocity axis rolls, the states P (roll rate) and R(yaw rate) are considered as input variables to the state equations. Other elements left as variable parameters to the program are velocity, altitude, angle of attack, and physical parameters of the aircraft model. With this set-up, the eigenvalues for both body axis and velocity axis rolls are obtained at various angles of attack and various roll rates.

A comparison of stability regions for body axis rolls and velocity axis rolls is then possible. For a given angle of attack the maximum roll rate can be determined before instability occurred.

The model of the aircraft has two types of longitudinal flight control systems, depending on whether the aircraft angle of attack is less than or greater than 20.4 degrees. It is of interest to the Air Force Flight Dynamics Laboratory to check the roll stability of the aircraft at various angles of attack using each of the two flight control system configurations separately. This is easily accomplished since the computer program for the linearized analysis (Appendix E) is designed to be as versatile as possible.

#### Bifurcation Analysis and Catastrophe Theory

This section gives only a brief overview of bifurcation analysis and catastrophe theory which is essential to the understanding of the nonlinear analysis in this thesis. A more complete explanation of these theories is contained in a report by Dr. Mehra, Mr. Kessel, and Dr. Carroll titled "Global Stability and Control Analysis of Aircraft at High Angles of Attack", (Ref 4).

Consider an example of a single nonlinear equation,

$$\frac{dx}{dt} = x^3 + (C_1)x + C_2 \quad (1.9)$$

where  $X$  is the state and  $C_1$  and  $C_2$  are the control parameters. A simplified explanation of bifurcation and catastrophe can be

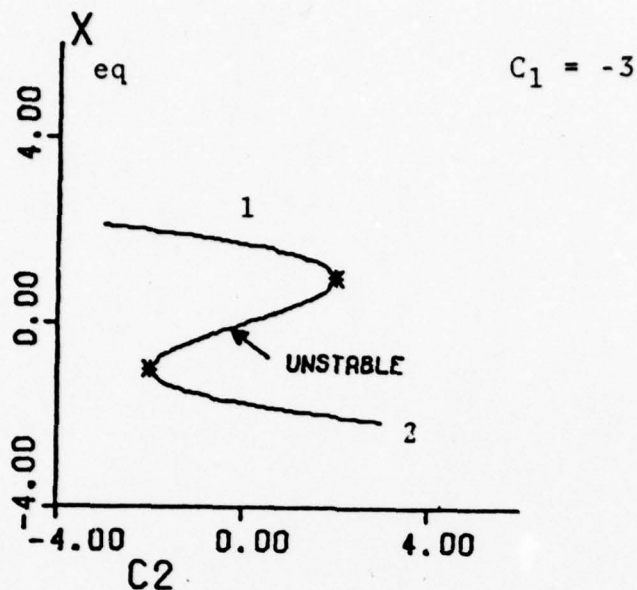


Fig. 1.1  $X_{eq}$  with bifurcation

in terms of this example nonlinear system. Figure 1.1 shows the solution of equation 1.9 for a fixed value of  $C_1$  and varying  $C_2$  from -3 to 3. The points on the curve in Figure 1.1 marked with the symbol \* are points of bifurcation. This is where the slope of the curve is infinite and occurs at the values of  $C_2 = -2$  and 2. Between these two points  $X_{eq}$  has 3 solutions -1 unstable and 2 stable. If  $C_2 = -3$  is the starting point and is then gradually increased,  $X_{eq}$  follows along branch 1 (a stable branch). Once  $C_2$  reaches a value slightly larger than 2, the value of  $X_{eq}$  jumps rapidly to a value on branch 2. This jumping is known as a catastrophe.

Figure 1.2 shows the solution to equation 1.9 for a different fixed value of  $C_1$  while varying  $C_2$  from -3 to 3. Here there are no bifurcation points and no catastrophes. This solution has a nice, smooth shape and is a more desirable solution than that of Figure 1.1.

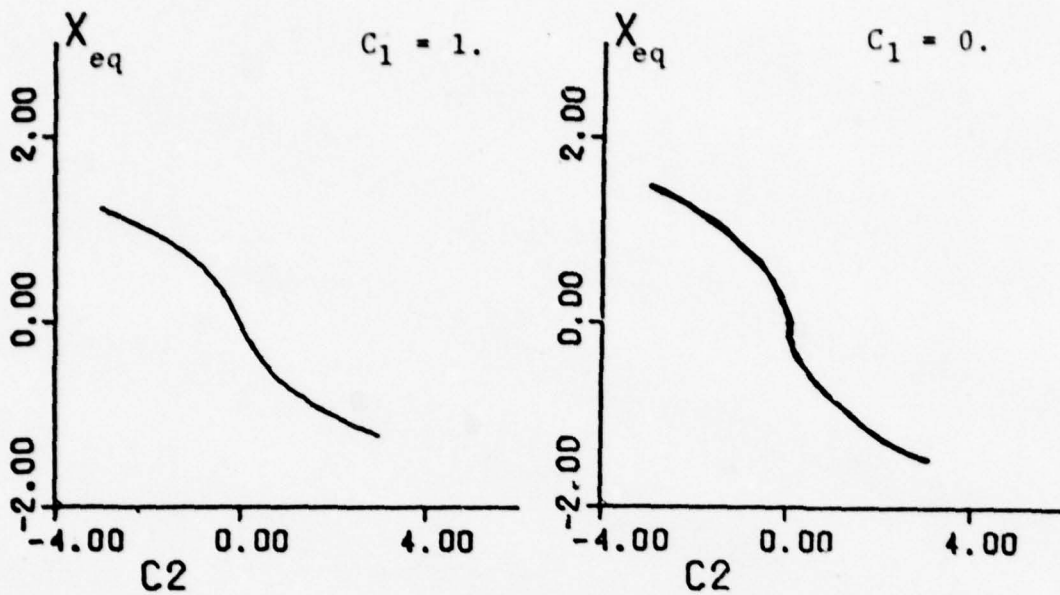


Fig. 1.2  $X_{eq}$  Without Bifurcation      Fig 1.3  $X_{eq}$  With Inflection Point

Figure 1.3 shows the solution to equation 1.9 for  $C_1 = 0$  while varying  $C_2$  from -3 to 3. Here there is a point where the slope is infinite but the control parameter does not reverse direction. This is known as an inflection point.

Figure 1.4 shows what is known as a cusp catastrophe which is representative of a third-order equation. For other orders of equations, there are other shapes and other types of catastrophes (Ref 4:24).

#### Method of Nonlinear Analysis

Starting with a nonlinear equation or set of simultaneous nonlinear equations and a set of control parameters, a computer program is needed that will solve all of the equations,

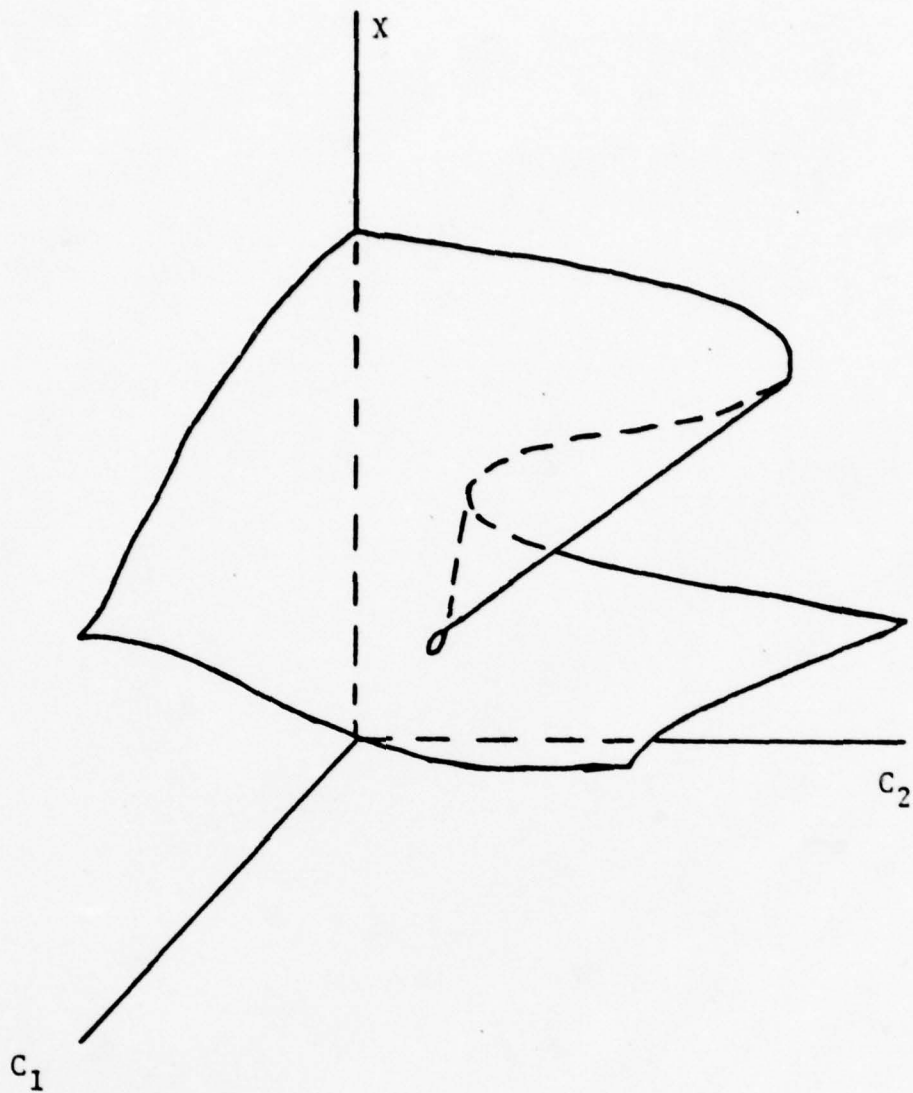


Fig. 1.4 Characteristic Representation of X Showing a Cusp Catastrophe.

given any combination of control parameters whereby the control parameters have specified upper and lower limits. A flow chart which represents what is needed in the program is shown in figure 1.5 (Ref 4). The first step is to set the control parameters of the equation(s) and all the other parameters needed in the program. The next step is to solve

the nonlinear equation(s) for a given pair of control parameters. The next step is to check whether the equation(s) has reached a bifurcation point, then increase or decrease the value of the control variables depending upon whether or not a bifurcation point has been reached. Checking for bifurcation points is accomplished by setting up the Jacobian matrix of the system, evaluated at the equilibrium values, and obtaining the systems eigenvalues. A bifurcation point occurs when an eigenvalue or set of eigenvalues passes through the imaginary axis. Continue all the steps above until all combinations of the control parameters have been considered. Finally, plot the solution to the equations(s) vs the control parameters.

#### Validity of Analysis

In the linearized analysis it can be said with reasonable assurance that the aircraft equations, stability derivatives, and flight control system are accurate and valid. The results show stability regions for both body axis rolls and velocity axis rolls at various angles of attack, and are very informative. The strongest support for these results is the similar trends found by the Air Force Flight Dynamics Laboratory, using a time history program for the same model aircraft.

For the case of a single nonlinear equation analysis, the program that shows the existence of bifurcation points and catastrophes gives results which have an accuracy of  $10^{-5}$ . The accuracy can easily be increased but is not necessary for the demonstration problem. To justify the solutions, a

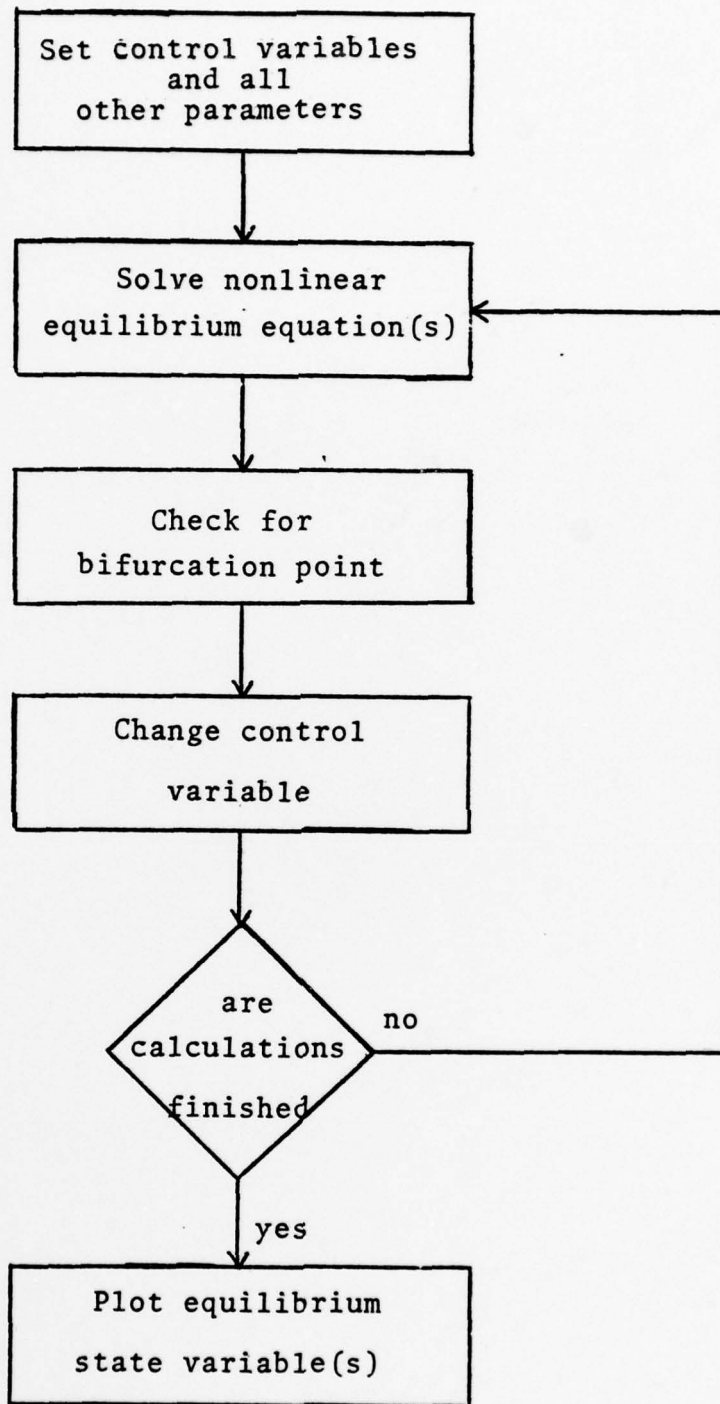


Fig. 1.5 Flow Chart for Nonlinear Equation(s) Solver.

separate analysis of the nonlinear equation is obtained by using a Texas Instruments 59 hand calculator. This method proves to be time consuming but it allows for a comparison of results. To further strengthen confidence in the developed program, the general shape of the solution to the equation is similar to that of an equation analyzed in (Ref. 4).

## II. Linear Analysis

### Reduced Linearized Model

To be sure that the aircraft model used is statically unstable, it is necessary to analytically check the stability of the model without a flight control system.

The equations of motion of an aircraft are

$$\Sigma F_x = m(\dot{U} + WQ - VR) \quad (2.1)$$

$$\Sigma F_y = m(\dot{V} + UR - WP) \quad (2.2)$$

$$\Sigma F_z = m(\dot{W} + VP - UQ) \quad (2.3)$$

$$\Sigma \Delta L = \dot{P}I_x - \dot{R}J_{xz} + QR(I_z - I_y) - PQJ_{xz} \quad (2.4)$$

$$\Sigma \Delta M = \dot{Q}I_y + PR(I_x - I_z) + (P^2 - R^2)J_{xz} \quad (2.5)$$

$$\Sigma \Delta N = \dot{R}I_z - \dot{P}J_{xz} + PQ(I_y - I_x) + QRJ_{xz} \quad (2.6)$$

where equations 2.1, 2.2., and 2.3 are the force equations and equations 2.4, 2.5, and 2.6 are the moment equations. Velocity (U) and roll rate (P) are assumed to be constant which eliminates equations 2.1 and 2.4. It is assumed that the xy plane of the aircraft is the plane of symmetry and the X-axis is selected as the symmetric axis. This allows the product of inertia ( $J_{xz}$ ) to be set to zero. Making the following assumptions

$$\alpha_0 = V_0 = W_0 = Q_0 = R_0 = 0 \quad (2.7)$$

where  $\alpha_o$ ,  $V_o$ ,  $W_o$ ,  $Q_o$ , and  $R_o$  are steady-state values, equations 2.2 and 2.3 are combined with their respective aerodynamic equations (Ref 1). Equations 2.4 and 2.5 are then substituted into equations 2.2 and 2.3.

The Laplace transform of the equations are

$$(a_1 s + a_o) \beta(s) + (b_2 s^2 + b_1 s + b_o)\alpha(s) = 0 \quad (2.8)$$

$$(c_2 s^2 + c_1 s + c_o) \beta(s) + (d_1 s + d_o)\alpha(s) = 0 \quad (2.9)$$

where the a's, b's, c's, and d's are constants which are listed in Appendix A. The characteristic equation produced from this model is

$$s^4 + A_1 s^3 + (A_2 P_o^2 + A_3) s^2 + (A_4 P_o^2 + A_5) s + (A_6 P_o^4 + A_7 P_o^2 + A_8) = 0 \quad (2.10)$$

where  $A_1, A_2, \dots, A_8$  are constants which are listed in Appendix A. The equation is purposely set up as a function of steady-state roll rate ( $P_o$ ) in order to study the effect that roll rate has on the aircraft. The full development of equation 2.10 is in Appendix A.

The characteristic equation is factored to obtain four roots-two dutch roll roots and two short period roots. These roots are plotted on a root locus as a function of roll rate. This plot not only shows the static stability of the aircraft but also shows the effect that roll rate has on the aircraft without a flight control system flying at

zero angle of attack. This method of root locus analysis was developed by Professor John Blakelock (Ref 1). This method is a helpful tool but contains too many assumptions for this particular aircraft model and is limited to straight and level flights only. A more versatile approach is needed.

### Full Linearized Model

The linear force equations and angular moment equations of motion are equations 2.1 thru 2.6. Again the velocity (U) is assumed constant. Since the perturbations are small, the second-order terms are assumed equal to zero.

In order for the aircraft model to be analyzed at various angles of attack and various roll rates-both in body axis and in velocity axis coordinates - the trimmed (steady-state) values of some of the aircraft states are left as variables. These variables include velocity (U), angle of attack ( $\alpha$ ), yaw rate (R), and roll rate (P). The trimmed values of pitch rate (Q), and y-axis velocity (V), are set to zero.

Combining equations 2.1 thru 2.6 with their aerodynamic force and moment equations, including the assumptions made, the following linearized aircraft equations are obtained (Ref 5):

$$\begin{aligned}
 mU_0 \dot{\beta} + mU_0 r - mU_0 P_0 \alpha - mU_0 P_0 p = \bar{q}s [C_{y\beta} \beta \\
 + C_{y_p} \left(\frac{b}{2U_0}\right) p + C_{y_r} \left(\frac{b}{2U_0}\right) r + C_{y_{\delta_f}} \delta_f + C_{y_{\delta_r}} \delta_r] \quad (2.11)
 \end{aligned}$$

$$\begin{aligned}
mU_o \dot{\alpha} + mU_o P_o \dot{\beta} - mU_o \dot{q} = \bar{q}s [C_{z_\alpha} \alpha + C_{z_\alpha} \dot{\alpha} \\
+ C_{z_q} \left(\frac{c}{2U_o}\right) q + C_{z_{\delta_s}} \delta_s] \quad (2.12)
\end{aligned}$$

$$\begin{aligned}
\dot{q} I_y + [P_o (I_x - I_z) - 2R_o J_{xz}] \dot{r} + [R_o (I_x - I_z) + 2P_o J_{xz}] \dot{p} = \\
\bar{q}s c [c_{m_\alpha} \alpha + C_{m_q} \left(\frac{c}{2U_o}\right) q + C_{m_\alpha} \left(\frac{c}{2U_o}\right) \dot{\alpha} + C_{m_{\delta_s}} \delta_s] \quad (2.13)
\end{aligned}$$

$$\begin{aligned}
\dot{p} I_x - \dot{r} J_{xz} + [R_o (I_z - I_y) - P_o J_{xz}] \dot{q} = \bar{q}s b [C_{\ell_\beta} \beta \\
+ C_{\ell_p} \left(\frac{b}{2U_o}\right) p + C_{\ell_r} \left(\frac{b}{2U_o}\right) r + C_{\ell_{\delta_f}} \delta_f + C_{\ell_{\delta_r}} \delta_r] \quad (2.14)
\end{aligned}$$

$$\begin{aligned}
\dot{r} I_z - \dot{p} J_{xz} + [P_o (I_y - I_x) + R_o J_{xz}] \dot{q} = \bar{q}s b [C_{n_\beta} \beta \\
+ C_{n_p} \left(\frac{b}{2U_o}\right) p + C_{n_r} \left(\frac{b}{2U_o}\right) r + C_{n_{\delta_f}} \delta_f + C_{n_{\delta_r}} \delta_r] \quad (2.15)
\end{aligned}$$

where  $U_o$ ,  $P_o$ , etc. are steady-state values and  $p$ ,  $r$ , etc. are small perturbations. Appendix B contains a more complete derivation of equations 2.10 thru 2.15. The values of the stability derivatives are a function of angle of attack. These values are listed in the computer program EIGEN in Appendix E and are given only for  $\alpha = 0, 10, 20$ , and  $25$  degrees. For the purpose of this thesis, these values of angle of attack are sufficient.

Since the aircraft model is statically unstable, it is necessary to augment the aircraft with a flight control system. The model also contains many nonlinear terms which cannot be ignored; therefore, both a longitudinal and a lateral flight control system are included. Figures 2.1 and 2.2 show a simplified block diagram of the longitudinal and lateral flight control systems used in this thesis. The flight control systems were supplied by the Air Force Flight Dynamics Laboratory.

The diagram of the longitudinal FCS contains two different flight control systems, the use of which depends on whether the angle of attack is greater than or less than 20.4 degrees. The lateral FCS contains a component known as an aileron-rudder interconnect (ARI). This component adds to the non-linearity of the model.

The equations for these flight control systems are developed in terms of physical variables -X1 thru X5 are the variables in the longitudinal FCS and Z1 thru Z4 are the variables in the lateral FCS. The flaperon, rudder, and stabilator displacements are also included as physical variables. The development and listing of these equations are in Appendix C.

The next step is to combine the aircraft equations with the longitudinal and lateral FCS and to arrange them in the following state variable form:

$$[A][\dot{\bar{X}}] = [A][\bar{X}] \quad (2.16)$$

where the 17 states are

$$[\bar{X}^T] = [\beta, \alpha, q, p, r, X_1, X_2, X_3, X_4, X_5, \delta_s, \delta_f, Z_1, Z_2, Z_3, Z_4, \delta_r] \quad (2.17)$$

The matrices are partitioned as follows:

$$[A] = \begin{bmatrix} A_{11} & A_{12} & A_{13} \\ A_{21} & A_{22} & A_{23} \\ A_{31} & A_{32} & A_{33} \end{bmatrix} \quad 17 \times 17 \quad (2.18)$$

$$[A_{12}] = [A_{13}] = [A_{23}] = [A_{32}] = 0$$

$$[A_{11}] = \begin{bmatrix} a_{11} & 0 & 0 & 0 & 0 \\ 0 & a_{22} & 0 & 0 & 0 \\ 0 & a_{32} & a_{33} & 0 & 0 \\ 0 & 0 & 0 & a_{44} & a_{45} \\ 0 & 0 & 0 & a_{54} & a_{55} \end{bmatrix} \quad 5 \times 5 \quad (2.19)$$

$$[A_{21}] = \begin{bmatrix} 0 & 0 & 0 & 0 & 0 \\ 0 & 0 & a_{73} & 0 & 0 \\ 0 & a_{82} & 0 & 0 & 0 \\ 0 & 0 & 0 & 0 & 0 \\ 0 & 0 & 0 & 0 & 0 \\ 0 & 0 & 0 & 0 & 0 \end{bmatrix} \quad (2.20)$$

$$[A_{22}] = \begin{bmatrix} a_{66} & 0 & 0 & 0 & 0 & 0 \\ 0 & a_{77} & 0 & 0 & 0 & 0 \\ 0 & 0 & a_{88} & 0 & 0 & 0 \\ a_{96} & a_{97} & a_{98} & a_{99} & 0 & 0 \\ a_{106} & 0 & 0 & a_{109} & a_{1010} & 0 \\ 0 & 0 & 0 & 0 & 0 & a_{1111} \end{bmatrix} \quad (2.21)$$

$$[A_{31}] = \begin{bmatrix} 0 & 0 & 0 & 0 & 0 \\ 0 & 0 & 0 & 0 & 0 \\ 0 & 0 & 0 & 0 & a_{145} \\ 0 & 0 & 0 & 0 & 0 \\ a_{161} & 0 & 0 & 0 & a_{165} \\ 0 & 0 & 0 & 0 & 0 \end{bmatrix} \quad (2.22)$$

$$[A_{33}] = \begin{bmatrix} a_{1212} & 0 & 0 & 0 & 0 & 0 \\ 0 & a_{1313} & 0 & 0 & 0 & 0 \\ 0 & a_{1413} & a_{1414} & 0 & 0 & 0 \\ 0 & 0 & a_{1514} & a_{1515} & 0 & 0 \\ 0 & 0 & 0 & a_{1615} & a_{1616} & 0 \\ 0 & 0 & 0 & 0 & 0 & a_{1717} \end{bmatrix} \quad (2.23)$$

$$[B] = \begin{bmatrix} B_{11} & B_{12} & B_{13} \\ B_{21} & B_{22} & B_{23} \\ B_{31} & B_{32} & B_{33} \end{bmatrix} \quad 17 \times 17 \quad (2.24)$$

$$[B_{23}] = [B_{32}] = 0$$

$$[B_{11}] = \begin{bmatrix} b_{11} & b_{12} & 0 & b_{14} & b_{15} \\ b_{21} & b_{22} & b_{23} & 0 & 0 \\ 0 & b_{32} & b_{33} & b_{34} & b_{35} \\ b_{41} & 0 & b_{43} & b_{44} & b_{45} \\ b_{51} & 0 & b_{53} & b_{54} & b_{55} \end{bmatrix} \quad 5 \times 5 \quad (2.25)$$

$$[B_{12}] = \begin{bmatrix} 0 & 0 & 0 & 0 & 0 & 0 \\ 0 & 0 & 0 & 0 & 0 & b_{211} \\ 0 & 0 & 0 & 0 & 0 & b_{311} \\ 0 & 0 & 0 & 0 & 0 & 0 \\ 0 & 0 & 0 & 0 & 0 & 0 \end{bmatrix} \quad 5 \times 6 \quad (2.26)$$

$$[B_{13}] = \begin{bmatrix} b_{112} & 0 & 0 & 0 & b_{116} & 0 \\ 0 & 0 & 0 & 0 & 0 & 0 \\ 0 & 0 & 0 & 0 & 0 & 0 \\ b_{412} & 0 & 0 & 0 & b_{416} & 0 \\ b_{512} & 0 & 0 & 0 & b_{516} & 0 \end{bmatrix} \quad 5 \times 6 \quad (2.27)$$

$$[B_{21}] = \begin{bmatrix} 0 & b_{62} & 0 & 0 & 0 \\ 0 & 0 & 0 & 0 & 0 \\ 0 & 0 & b_{83} & 0 & 0 \\ 0 & 0 & 0 & 0 & 0 \\ 0 & 0 & 0 & 0 & 0 \\ 0 & 0 & 0 & 0 & 0 \end{bmatrix} \quad (2.28)$$

6x5

$$[B_{22}] = \begin{bmatrix} b_{66} & 0 & 0 & 0 & 0 & 0 \\ 0 & b_{77} & 0 & 0 & 0 & 0 \\ 0 & 0 & b_{88} & 0 & 0 & 0 \\ b_{96} & b_{97} & b_{98} & b_{99} & 0 & 0 \\ 0 & 0 & 0 & b_{109} & 0 & 0 \\ 0 & 0 & 0 & 0 & b_{1110} & b_{1111} \end{bmatrix} \quad (2.29)$$

6x6

$$[B_{31}] = \begin{bmatrix} 0 & 0 & 0 & b_{124} & 0 \\ 0 & b_{132} & 0 & b_{134} & 0 \\ 0 & 0 & 0 & 0 & 0 \\ 0 & 0 & 0 & 0 & 0 \\ 0 & b_{162} & 0 & b_{164} & b_{165} \\ 0 & 0 & 0 & 0 & 0 \end{bmatrix} \quad (2.30)$$

6x5

$$[B_{33}] = \begin{bmatrix} b_{1212} & 0 & 0 & 0 & 0 & 0 \\ 0 & b_{1313} & 0 & 0 & 0 & 0 \\ 0 & 0 & b_{1414} & 0 & 0 & 0 \\ 0 & 0 & b_{1514} & b_{1515} & 0 & 0 \\ 0 & 0 & 0 & b_{1615} & b_{1616} & 0 \\ 0 & 0 & 0 & 0 & b_{1716} & b_{1717} \end{bmatrix} \quad (2.31)$$

6x6

The elements for matrices A and B are from the airplane equations and flight control system and are listed in the computer program EIGEN in Appendix E.

The computer program EIGEN is set up to solve for the eigenvalues of the following system

$$\dot{\bar{X}} = [A^{-1}B] \bar{X} \quad (2.32)$$

which are obtained from equation 2.16.

The first step in the use of the program is to input the desired trim conditions of the aircraft. The inputs include velocity, altitude, moments of inertia, product of inertia, angle of attack, roll rate, yaw rate, surface area, chord, wing span, air pressure, static pressure and mass of the aircraft. The units of these inputs are listed in Appendix E.

Once this is done, the program solves for the eigenvalues and/or eigenvectors of matrix  $[A^{-1}B]$ . The first set of runs is set up to solve for the eigenvalues and eigenvectors of the system, both with and without a flight control system, for a given angle of attack and zero roll rate. This permits the determination of where the eigenvalues originate. Without feedback, the eigenvalues of the flight control system are easy to identify since the FCS is set up in physical variable form. This leaves five eigenvalues unidentified. At this point the eigenvectors are used to identify the remaining five aircraft eigenvalues: Two



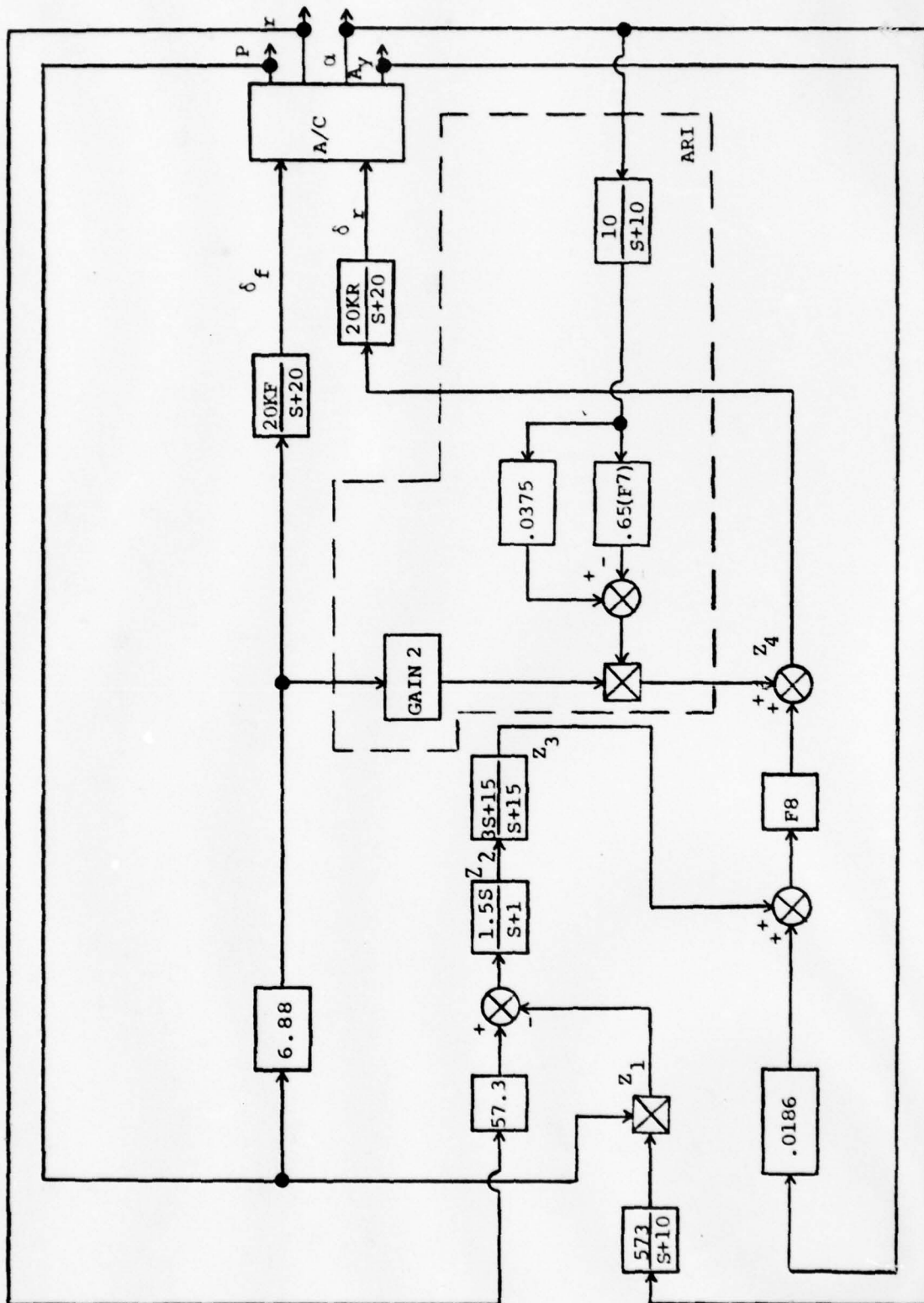


Fig. 2.2 Lateral Flight Control System with ARI.

longitudinal eigenvalues (short period roots) and three lateral eigenvalues (two dutch roll roots and one rolling mode root).

After identifying the seventeen eigenvalues of the aircraft with feedback as either longitudinal or lateral, the next step is to map the longitudinal eigenvalues, with and without feedback, on a graph. The same is done with the lateral eigenvalues. An example is shown in Appendix D. This mapping makes it easy to identify each of the eigenvalues of the aircraft with feedback. A comparison with military specifications is made for the short period, dutch roll, and rolling mode roots in order to prove that the model used is a valid example of a fighter-type aircraft (Ref 6).

At this point, a question arises as to whether the flight control system can be reduced, thus simplifying the analysis. Due to the nonlinearities in the aircraft it is necessary to retain both the complete longitudinal and lateral-directional FCS. One possibility is the removal of the aileron-rudder interconnect (ARI). Without the ARI one of the physical states (F4) in the lateral FCS can be eliminated. An analysis of the short period, dutch roll, and rolling mode roots of the aircraft with its FCS is performed both with and without the ARI. This is done at 0, 10, 20, and 25 degrees angle of attack. The results are given in table 4.1 with the conclusions given in Chapter V.

The next step is to study the effect that angle of attack has on the aircraft. This is done by obtaining the

the short period, dutch roll, and rolling mode roots of the aircraft with FCS at various angles of attack. The computer program EIGEN is then set up to solve for the eigenvalues of the aircraft, with FCS, while performing rolls. The program is set up to solve for the eigenvalues while the roll rate,  $p$ , is incremented from 0 to 7 rad/sec. The first step is to compare the full model with the reduced model. For comparison, the full model is analyzed with inputs of zero angle of attack, zero product of inertia, and zero feedback. Since the reduced model has only short period and dutch roll roots, these are the only modes which can be compared.

A stability analysis of body axis rolls vs. velocity axis rolls can now be conducted. To perform body axis rolls, the yaw rate,  $r$ , is set to zero while the roll rate,  $p$ , is incremented from 0 to 7 rad/sec. This allows the aircraft to roll about it's own X-axis. It is not necessary to analyze rolls beyond 7 rad/sec since the A. F. Flight Dynamics Laboratory is not interested in an analysis beyond that point. To perform velocity axis rolls, the roll rate,  $p$ , is incremented from 0 to 7 rad/sec, while the yaw rate,  $r$ , is set as a function of roll rate and angle of attack:

$$r = p \tan \alpha \quad (2.33)$$

The combination of  $p$  and  $r$  allows the aircraft to roll about it's velocity vector.

The program EIGEN is then used to scan the eigenvalues for roll rates over the range of 0 to 7 rad/sec about the body axis and the velocity axis, and to record the areas of stability and instability. This is done at various angles of attack. Of primary interest is the case of high angles of attack- 20 and 25 degrees. Plots are made with body axis rolls, velocity axis rolls, and lines of instability for various angles of attack.

The final point of interest with the linear analysis is whether it is necessary to have two longitudinal flight control systems, depending on whether the angle of attack is less than or greater than 20.4 degrees. A plot showing lines of instability at angles of attack of 0, 10, 20, and 25 degrees is available with the dual longitudinal flight control systems. A new set of plots (see Chapter IV) is then run at these same angles of attack, but only one of the longitudinal flight control systems is incorporated. This is repeated for the other flight control system.

### III. Nonlinear Analysis

#### Single Nonlinear Equation

In order to use the ideas of bifurcation analysis and catastrophe theory a computer program is needed to perform the steps shown in the flow chart of Figure 1.5. To simplify the programming, a single nonlinear equation is analyzed first. The nonlinear equation selected (Ref 4:15) is

$$f = \frac{dx}{dt} = x^3 + C_1x + C_2 \quad (3.1)$$

where  $X$  is the variable and  $C_1$  and  $C_2$  are control parameters.

The first step is to set the control parameters to some desired initial condition. For the purpose of this thesis, the control parameters are varied from -3 to 3; therefore, the initial values for both control parameters are set to -3.

The next step is to solve for the equilibrium value of  $X$  ( $X_{eq}$ ), given the values of both control parameters. An AFIT subroutine NS01A is selected to solve for  $X_{eq}$ . This subroutine is available in the ASD Computer Center library at Wright-Patterson AFB.

In order to check for a bifurcation point the derivative of equation 3.1 is needed, given the equilibrium value of  $X_{eq}$ :

$$g = \left. \frac{\partial F}{\partial X} \right|_{X_{eq}} = 3X_{eq}^2 + C_1 \quad (3.2)$$

where  $g$  is the linearized system of  $F$ . If  $g$  is less than

zero, the equilibrium value of  $X$  is stable. If  $g$  is greater than zero, the equilibrium value of  $X$  is unstable. If  $g$  equals zero, a bifurcation point is encountered.

The digital computer program is set up with two loops- an inner loop which increments the control parameter  $C_2$  and an outer loop which increments the control parameter  $C_1$ . In the inner loop, if  $g$  is not equal to zero,  $C_1$  is set to  $C_2 + \Delta C_2$ , where  $\Delta C_2$  is a small increment of  $C_2$ . If  $g$  is equal to zero, the sign of  $\Delta C_2$  is changed and then  $C_2$  is set to  $C_2 + \Delta C_2$ . Everytime a bifurcation point is encountered, the sign of  $\Delta C_2$  is changed. For example, if  $C_2$  starts at -3 and is increased by a small amount after each equilibrium value of  $X$  is obtained,  $C_2$  is increased until a bifurcation point is encountered. At this point  $C_2$  would start decreasing until another bifurcation point is met; then  $C_2$  would start increasing again. This process continues until  $C_2$  eventually reaches it's maximum value.

When  $C_2$  completely covers the range of -3 to 3, the outer loop of the digital program is engaged. This loop resets  $C_2$  to -3 and increments  $C_1$ . Here the process in the inner loop starts again. Another way of explaining the computer program is that  $X_{eq}$  is obtained as a function of  $C_2$  with  $C_1$  set to a constant. This is the inner loop. All the outer loop does is increase the value of  $C_1$  and returns to the inner loop. Once the range of -3 to 3 for  $C_2$  is covered, the process of solving for  $X_{eq}$  is completed.

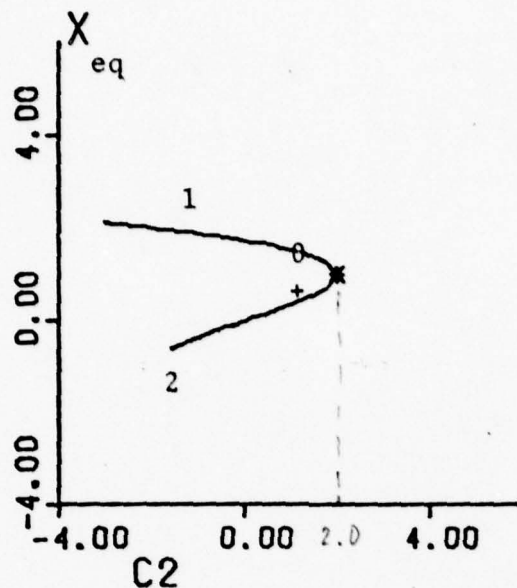


Fig. 3.1 Shifting of  $X_{eq}$  at Bifurcation Point.

The outputs of the computer program include a listing of  $X_{eq}$  for values of  $C_1$  and  $C_2$ , the residuals of  $X_{eq}$ , and the sum of the squares of the residuals of  $X_{eq}$ .

Since the subroutine NS01A solves for only one equilibrium value of  $X$  at a time, it is necessary to make sure that the solution of equation 3.1 isn't repeated when  $\Delta C_2$  changes sign. To avoid this, the next guess of  $X_{eq}$  is changed to a value closer to the next nearest value of  $X_{eq}$ . An illustration of this is shown in Figure (3.1) where \* represents a bifurcation point and 0 represents a solution of equation 3.1 already known. Once  $C_2$  is incremented, the subroutine NS01A uses the present value of  $X_{eq}$  as the guess to compute the next value of  $X_{eq}$ . At  $C_2 = 2$  a bifurcation point is reached and therefore  $C_2$  is decremented. In order to prevent  $X_{eq}$  from retracing branch (1), it is necessary to adjust the

next guess of  $X_{eq}$  to point (+) which is closer to branch (2). This allows the program to solve for  $X_{eq}$  on branch (2). The computer program which performs all of the above steps is called NONLIN and is listed in Appendix E.

The final phase of the program is to plot a series of two-dimensional arrays showing  $X_{eq}$  vs  $C_2$  with  $C_1$  set to a desired value. These plots and the listing of  $X_{eq}$  are compared to known solutions of equation 3.1.

### Coupled Nonlinear Equations

The next step in the development of the nonlinear analysis technique is to modify NONLIN to solve for two nonlinear coupled equations. The equations used are

$$\frac{dx_1}{dt} = x_1^3 + C_1 x_2 + C_2 \quad (3.3)$$

$$\frac{dx_2}{dt} = x_2^3 + C_2 x_1 + C_1 \quad (3.4)$$

The part of NONLIN which checks for bifurcation points is the only part which needs modification. Once the equilibrium values of  $X_1$  and  $X_2$  are obtained from NS01A, the eigenvalues of the Jacobian matrix are derived. Since the inverse Jacobian matrix is available from NS01A, it is easy to solve for the eigenvalues of the system. Whenever any of the eigenvalues are zero, a bifurcation point is reached and the sign of the increment of the inner loop control parameter ( $C_2$ ) is changed. It is not possible to know whether  $X_1$ ,  $X_2$ , or

both have reached a bifurcation point. This problem isn't considered important since the state which doesn't hit a bifurcation point will only backtrack on the same solution. Once the entire range of  $C_2$  is covered, all the values of  $X_{1eq}$  and  $X_{2eq}$  have been derived. The two-dimensional plots are set up to give the solutions of  $X_{1eq}$  vs  $C_2$  and  $X_{2eq}$  vs  $C_2$  for a selected value of  $C_1$ , of  $C_1$ , where  $X_{1eq}$  and  $X_{2eq}$  are the equilibrium solutions of the equations.

#### IV. Results

##### Linear Analysis

The results of the reduced linearized model for the aircraft alone are shown on a graph (Fig 4.1). At zero roll rate the short period roots are real (-0.57 and +0.34). And the dutch roll roots are complex conjugates (-0.08 + j1.06). As the roll rate is increased the short period roots move away from the imaginary axis until  $P = 0.6$  rad/sec. At this point the short period roots move back toward the imaginary axis. At  $P = 1.23$  rad/sec. the aircraft model becomes stable because both short period roots are now negative. At  $P = 1.25$  rad/sec. the short period roots change from two real roots to a pair of complex conjugate roots. As  $P$  continues increasing, the short period roots move away from both the real and imaginary axis. The dutch roll roots remain complex and move away from the real axis but toward the imaginary axis. The plot of Figure 4.1 contains the roots for values of roll rate from 0 to 12 rad/sec.

The results of the aircraft with the FCS, showing the effect of variations in angle of attack (AOA), are in Table (4-1). This table shows the results for the model both with and without the aileron rudder interconnect (ARI). The short period roots combine with a pair of longitudinal FCS roots to form two pairs of complex conjugate roots. Their damping ratios and natural frequencies remain about the same for 0, 10, and 20 degrees AOA. At 25 degrees AOA, the short period roots break away from the longitudinal FCS and form a single pair of complex conjugate roots and two real roots. The rolling mode root

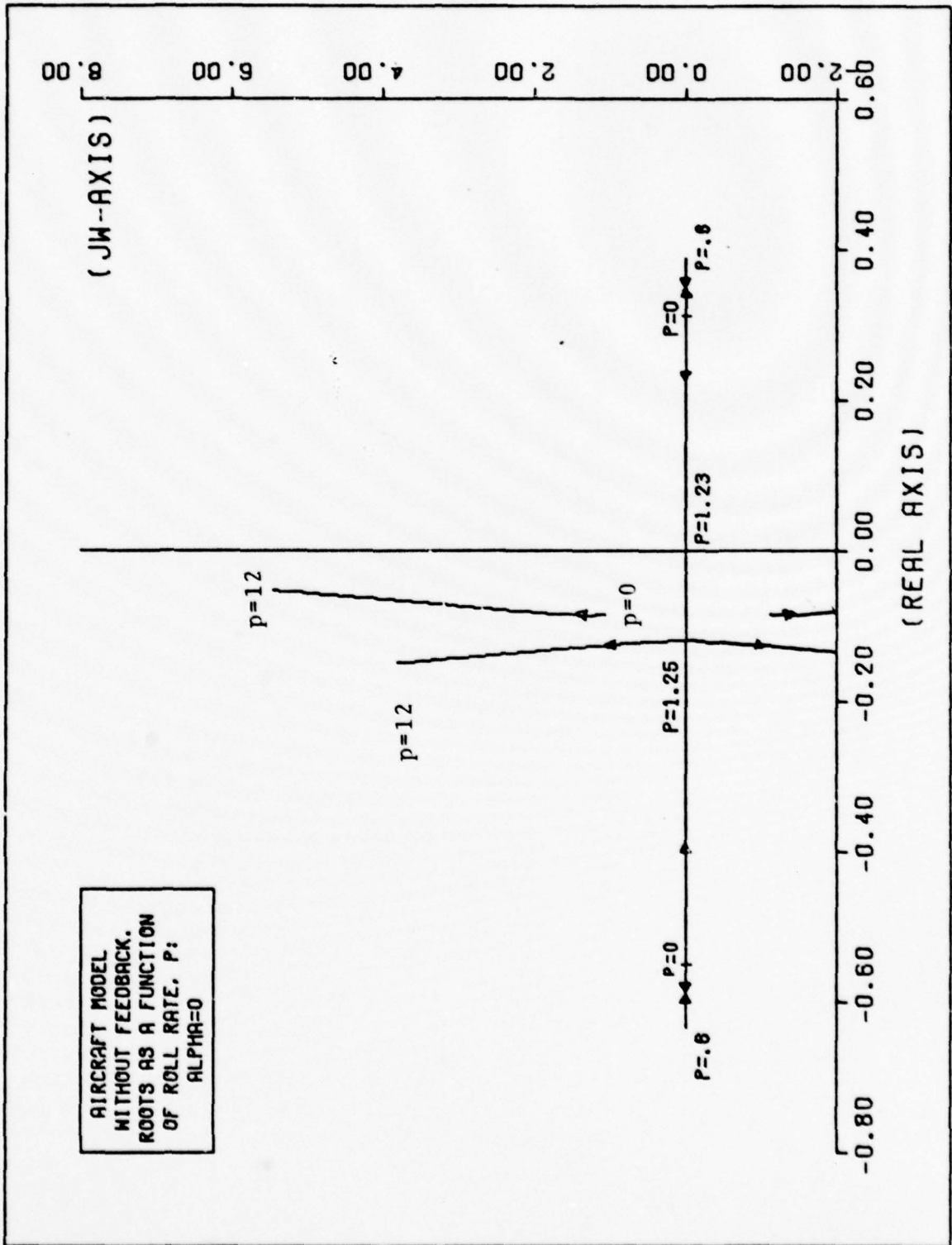


Fig 4.1 Root Locus for Reduced Linear Model

combines with a longitudinal FCS root to form a pair of complex conjugate roots. At 10, 20, and 25 degrees AOA the two complex roots break into one real FCS root and one real rolling mode root.

The results for the aircraft model with the ARI are basically the same as for the aircraft without the ARI as shown in Table (4.1). The differences show up in the roots of the lateral FCS. Without the ARI, one of the eigenvalues from the lateral FCS is unstable for a straight and level flight. With the ARI connected, the lateral FCS becomes stable. From this point on, the results presented in this report include the aircraft model with the aileron-rudder interconnect.

For a category A flight phase with level one flying quality, the minimum short period damping ratio ( $\rho_{sp}$ ) is 0.35, the minimum dutch roll damping ratio ( $\rho_{DR}$ ) is 0.19, and the minimum dutch roll natural frequency ( $\omega_{DR}$ ) is 1.0 rad/sec. (Ref 6). These are the specifications for a fighter type aircraft under highly maneuverable flight conditions. For all angles of attack the short period damping ratios meet the specifications. The dutch roll damping ratios also meet the specifications. The dutch roll natural frequencies fall short of the specifications at 0 and 25 degrees AOA but are within specifications at 10 and 25 degrees AOA.

		DUTCH ROLL ROOTS	$\omega_{nDR}$	$\rho_{DR}$	SHORT PERIOD + LONG-FCSROOTS	$\omega_{nSP+FCS}$	$\rho_{SP+FCS}$	ROLLING MODE and/or LONG-FCS ROOTS
WITHOUT ARI	0	$-.1749+j.9445$	.96	.18	$-1.45+j2.535$	2.92	.496	$-1.233+j.1965$
	10	$-.361+j1.14$	1.19	.30	$-1.47+j2.3$	2.73	.54	$-.811+j0$
	20	$-.3764+j1.137$	1.19	.314	$-1.198+j2.1$	2.42	.495	$-.3714+j0$
	25	$-.193+j.764$	.79	.25	$-.412+j.675$	.79	.52	$-.236+j0$
WITH ARI	0	$-.2028+j.8157$	.84	.24	$-1.45+j2.534$	2.92	.497	$-1.311+j.0657$
	10	$-.45+j1.06$	1.15	.39	$-1.47+j2.3$	2.73	.54	$-.8042+j0$
	20	$-.446+j1.05$	1.14	.39	$-.419+j.689$	.81	.52	$-.3246+j0$
	25	$-.275+j.7035$	.76	.36	$-1.099+j2.45$	2.42	.5	$-.1574+j0$

Table 4.1 Variations in AOA, With and Without the Aileron Rudder Interconnect.

The results of the reduced linearized model are then compared with the results of the full linearized model. It is found that both models produce a pair of complex conjugate dutch roll roots ( $-0.084 \pm j 1.06$  for the reduced model and  $-1.32 \pm j 1.06$  for the full model) and a pair of real short period roots ( $-0.567$  and  $0.334$  for the reduced model and  $-0.664$  and  $0.176$  for the full model).

To show the results for body axis rolls vs velocity axis rolls the regions of instability are needed. Figure 4.2 shows how these lines relate to each other for various angles of attack. The area to the right of the lines is where the rolling mode root is unstable. This is for the range of 0 to 7 rad/sec. roll rate.

Figure 4.3 shows the results of body axis rolls vs velocity axis rolls at 0, 10, 20, and 25 degrees AOA. This is with the dual longitudinal FCS. At 0 degrees AOA, a body axis roll is the same as a velocity axis roll. This is apparent from equation 3.1. Figure 4.4 shows the same results using the longitudinal FCS for angles of attack less than 20.4 degrees. Figure 4.5 shows the same results using the longitudinal FCS for angles of attack greater than 20.4 degrees.

The results contained in Figures 4.3 and 4.4 are compiled in Table 4.2. At 0 degrees AOA the aircraft is unstable at 1.8 rad/sec. roll rate for the dual FCS. At 10 degrees AOA the aircraft is unstable at 2.0 rad/sec roll rate for a body axis roll and at 2.14 rad/sec roll rate for a velocity axis roll. At 20 degrees AOA, the aircraft is unstable at 2.4 rad/sec roll rate for a body axis roll and at 3.29 rad/sec roll rate for a velocity axis roll. At 25 degrees AOA, the

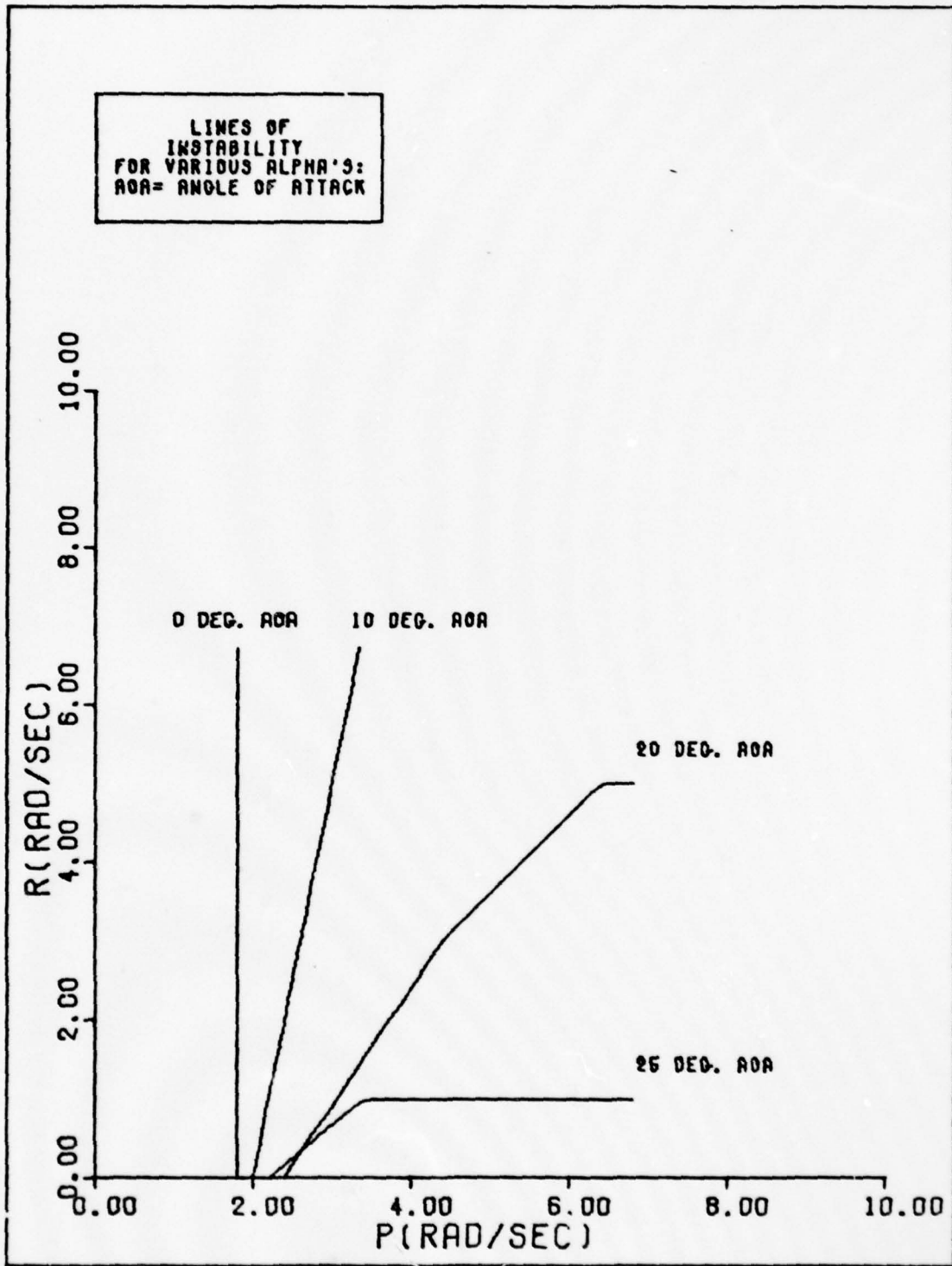


Fig. 4.2 Lines of Instability for Variations in AOA.

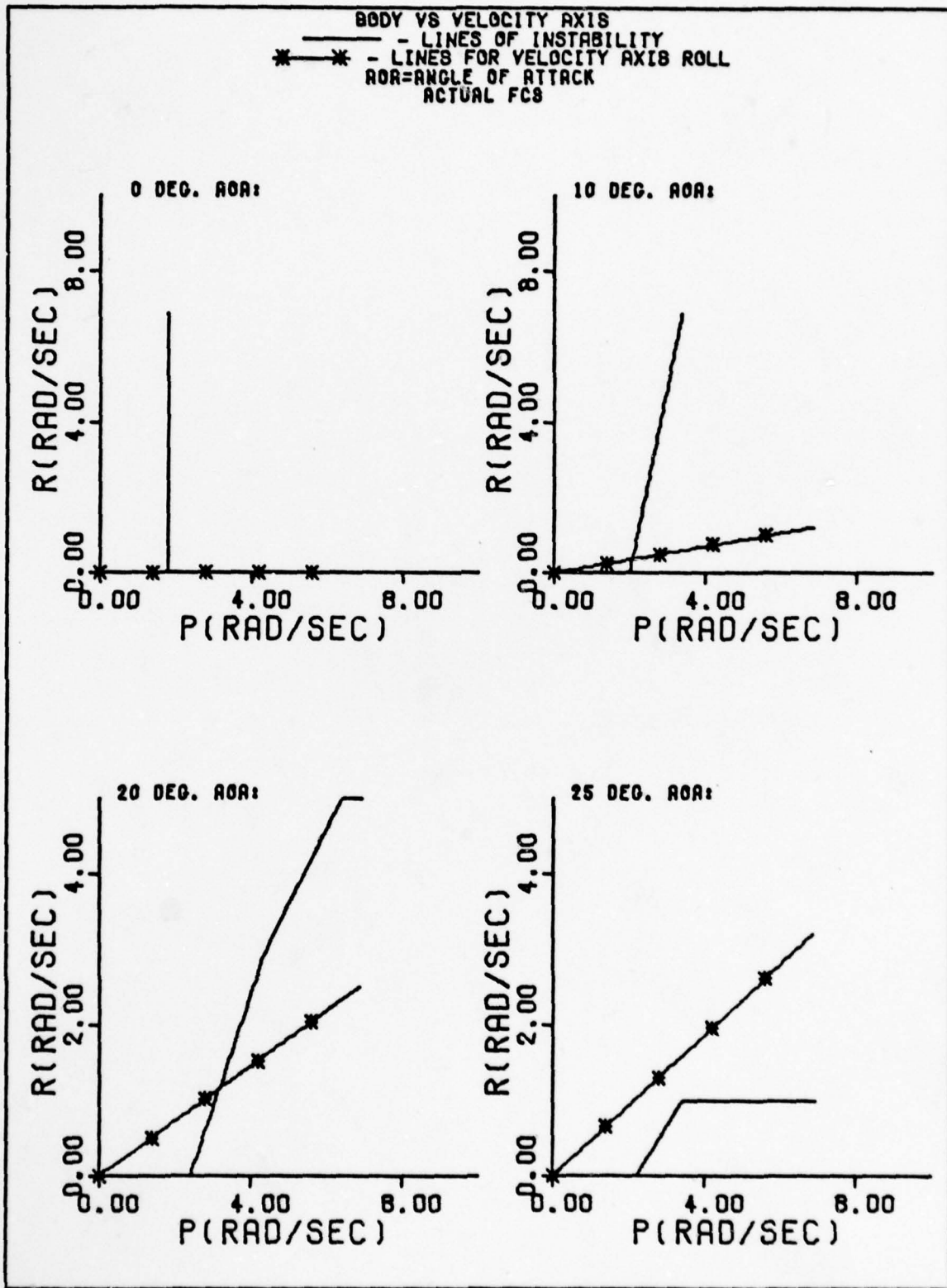


Fig. 4.3 Body Axis vs Velocity Axis Rolls with Dual Long. FCS.

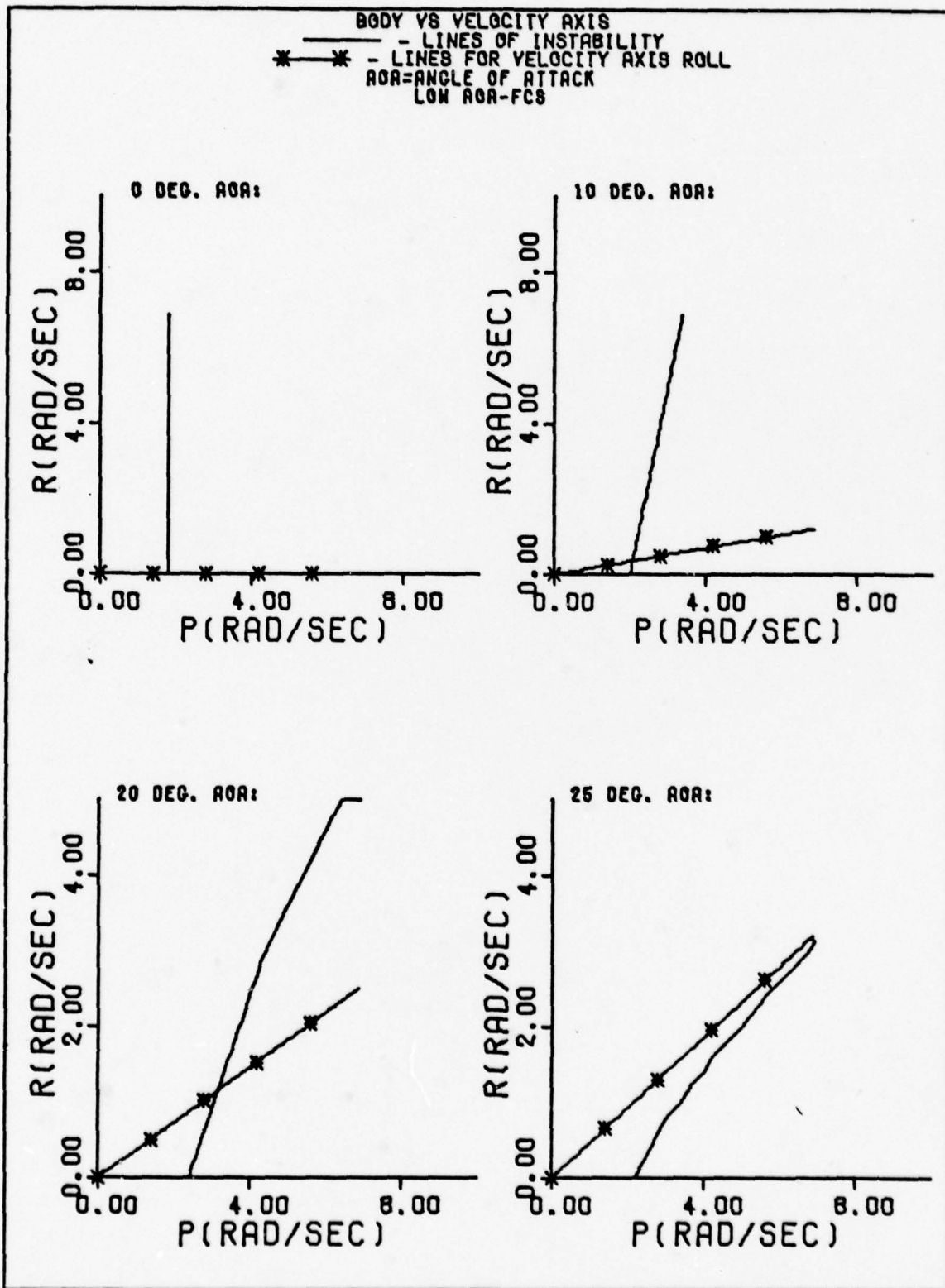


Fig. 4.4 Body Axis vs Velocity Axis Rolls with Low AOA Long. FCS.

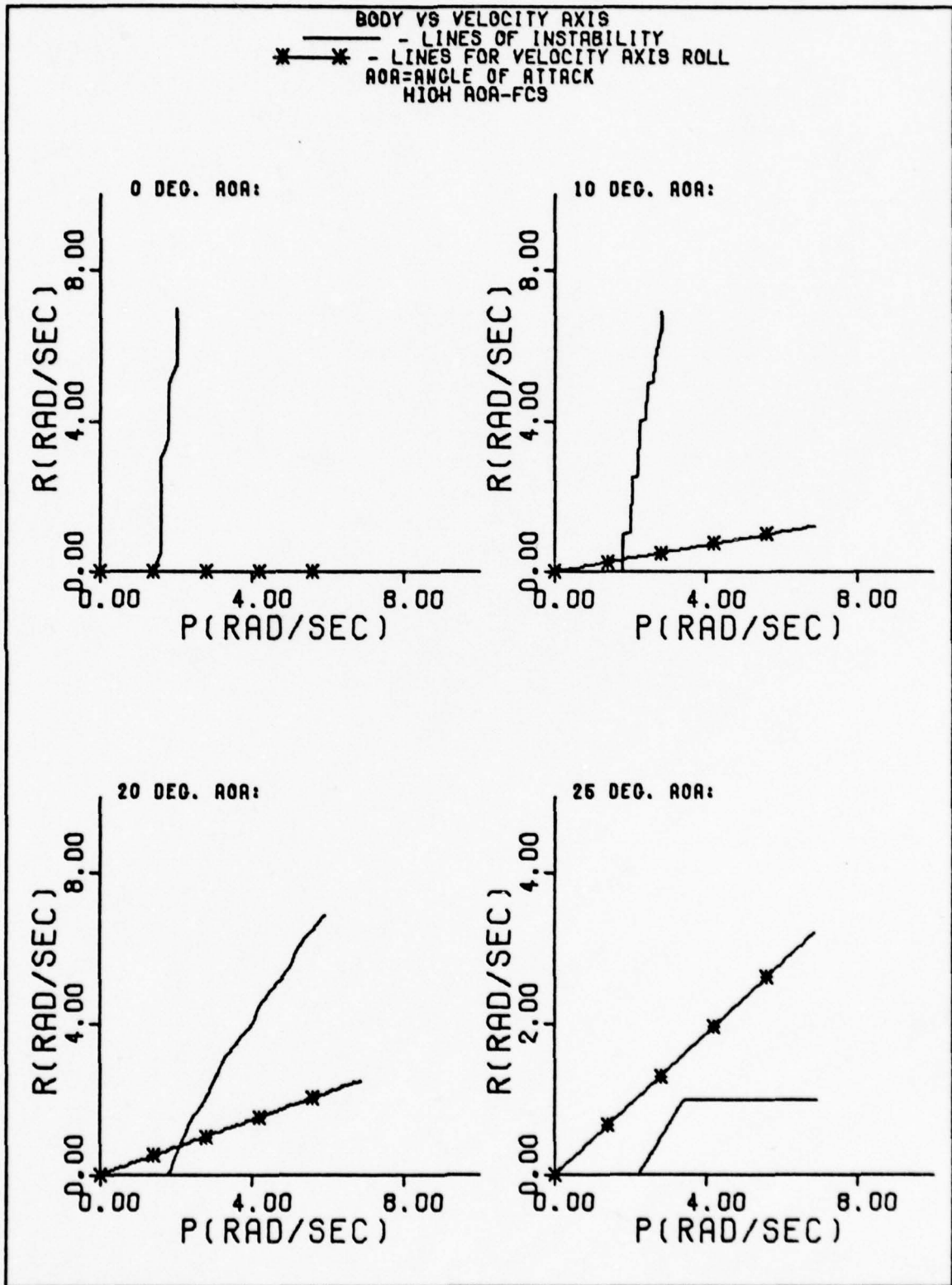


Fig. 4.5 Body Axis vs Velocity Axis Rolls with High AOA Long. FCS.

ROLL RATE WHERE AIRCRAFT GOES UNSTABLE (RAD/SEC.)						
$\alpha$ (DEGS)	Dual Longitudinal FCS		HIGH AOA Longitudinal FCS		LOW AOA Longitudinal FCS	
	Body	Velocity	Body	Velocity	Body	Velocity
	Axis roll	Axis roll	Axis roll	Axis roll	Axis roll	Axis roll
0	1.8	1.8	1.4	1.4	1.8	1.8
10	2.0	2.14	1.8	1.86	2.0	2.14
20	2.4	3.29	1.8	2.14	2.4	3.29
25	2.2	>7.0	2.2	>7.0	2.2	> 7.0

Table 4.2 Occurance of Instability for Aircraft with Various FCS's.

aircraft is unstable at 2.2 rad/sec roll rate for a body axis roll and remains stable to 7.9 rad/sec roll rate for a velocity axis roll. In all cases the aircraft remains stable for larger velocity axis rolls than for body axis rolls. As the AOA increases, the aircraft remains stable for larger values of roll rate for velocity axis rolls. At 25 degrees AOA the aircraft is stable up to 8.6 rad/sec. roll rate for a velocity axis roll. These same trends were found by the Air Force Flight Dynamics Laboratory in their time history evaluations of the same model.

A comparison of the three flight control system configurations show that the high AOA longitudinal FCS gives poorer results for body axis and velocity axis rolls at 0, 10, and 20 degrees AOA when compared with the dual longitudinal FCS. The results also show that the low AOA longitudinal FCS produces instabilities

at smaller roll rates than the dual longitudinal FCS when at 25 degrees AOA. These results are shown in Table 4.2.

### Nonlinear Analysis

The results of the single nonlinear equation are shown in Figure 4.6 which is produced by use of the computer program NONLIN. Bifurcation points are encountered for  $C_1 < 0$  and cusp catastrophes occur. These results are shown to be correct when compared with the results obtained with a Texas Instruments 59 hand calculator. The characteristic shape of the curve of  $X$  vs  $C$  is similiar to that shown in a report by Dr. Mehra, Mr. Kessel, and Dr. Carroll (Ref 4:17).

When the two coupled equations are tried, a bifurcation point is never encountered. While incrementing the control parameter  $C_2$ , an eigenvalue does cross the imaginary axis which is an indication that  $X_1$ ,  $X_2$ , or both  $X_1$  and  $X_2$  has reached a bifurcation point. The data shows that there is no indication of a bifurcation point. There also is no indication of an inflection point.

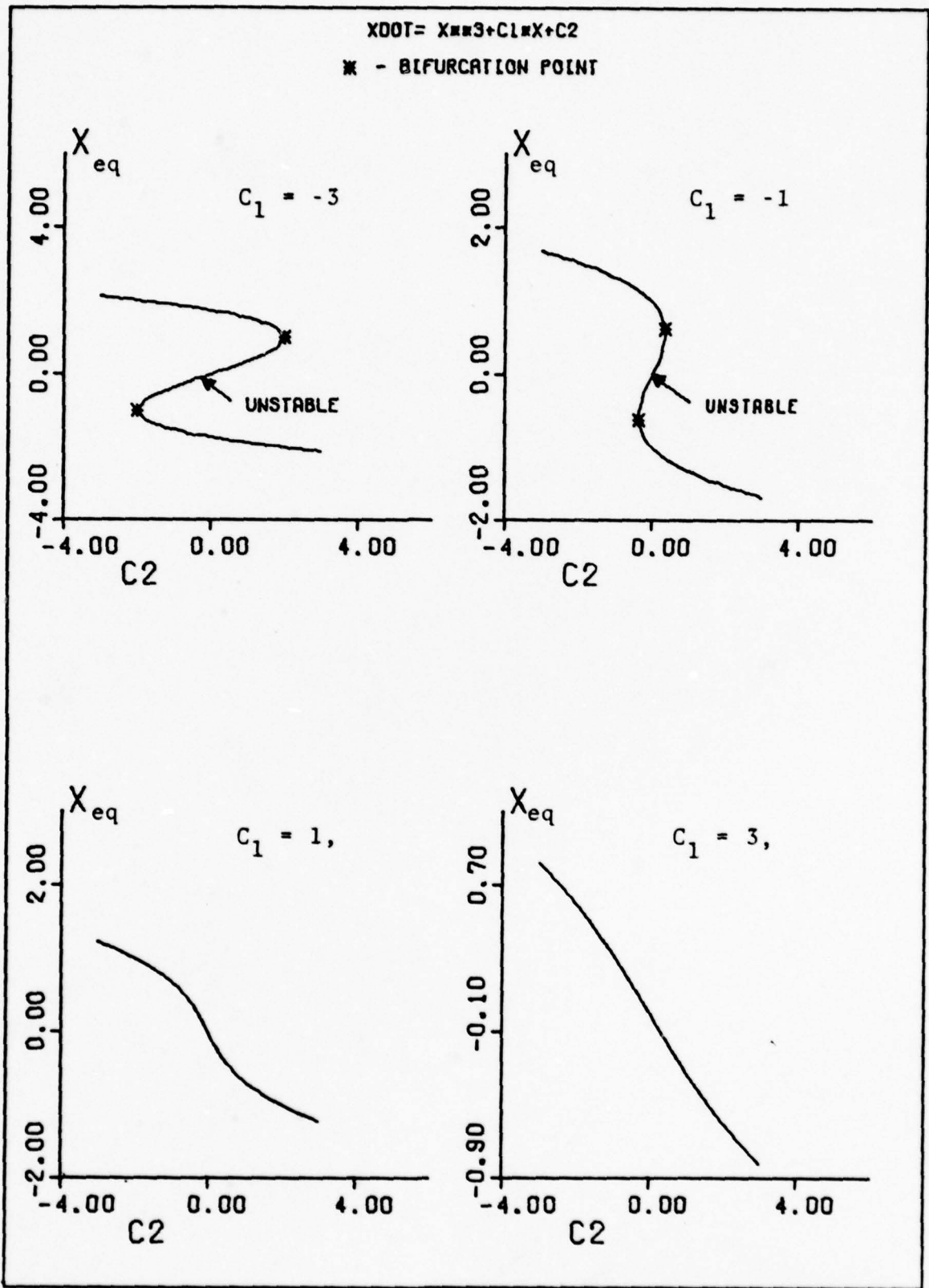


Fig. 4.6  $X$  vs  $C_2$  for Various Values of  $C_1$ .

## V. Conclusions and Recommendations

### Linear Analysis Conclusions

Since the lateral FCS is statically unstable without the aileron rudder interconnect (ARI) it is obvious that the ARI is a necessary part of the model's FCS and cannot be excluded.

A comparison of the model's roots with specifications shows that the aircraft model used in this analysis is representative of a fighter-type aircraft.

When the reduced model is compared to the full model, it is observed that the short period roots and dutch roll roots are closely related but different. The dutch roll roots are different, primarily because the aerodynamics of the M-moment equation and the Z-force equation are neglected in the reduced model. The short period roots are different, primarily because the aerodynamics of the N-moment equation are neglected.

In the comparison of body axis rolls vs velocity axis rolls, the aircraft remains stable for larger roll rates when it rolls about its velocity vector. The comparison of the three sets of longitudinal flight control systems show the necessity for the dual longitudinal FCS. This is not to say that there doesn't exist a single FCS which gives better roll rate performance. The results show that the combination of the two longitudinal flight control systems performs better over the range of 0 to 25 degrees AOA than when just one of the longitudinal flight control systems is used.

### Linear Analysis Recommendations

The linear analysis in this thesis has produced an acceptable linear model of a statically unstable fighter-type aircraft. This thesis has also shown that the aircraft becomes unstable when performing rolls. The elimination of the problem has not been looked into.

One possible procedure would be to set up a computer program that takes the state space model of the aircraft and produces time responses for any state to a desired input. This has been done in a computer program called TOTAL which is available in the Air Force Institute of Technology program library. The dimension statements in TOTAL presently limit the model to no more than ten states. Since this model has seventeen states, a change of the dimension statements programming is needed.

Once this is done, a study of the influence that various feedback components have on the states of the model can be performed. This would possibly help find the cause of the loss of control. The final step would be to eliminate the loss of control without depreciating the performance of the aircraft.

### Nonlinear Analysis Conclusions

The analysis of the single nonlinear equation has provided a good initial step in the development of a computer program for applying bifurcation analysis and catastrophe theory to a control problem. The coupled equations used proved to be unsatisfactory for this analysis. A more indepth study is required at this point.

### Nonlinear Analysis Recommendations

This study has laid the ground work for using bifurcation analysis and catastrophe theory to analyze nonlinear equations. It is possible that this same approach could be used to analyze the nonlinear aircraft equations of motion. What is needed is a computer program that uses the same principles outlined in Figure 1.5 and is capable of solving the aircraft equations. From here, a study of the influence that various feedback components have on the solutions to the aircraft equations could be performed. Finally, determine where the loss of control is coming from while performing rolls and then eliminate the problem without depreciating the overall performance of the aircraft.

## Bibliography

1. Blakelock, John H., Automatic Control of Aircraft and Missiles. New York: Wiley and Sons, 1965.
2. D'Azzo, John J. and Constantine H. Houpis, Linear Control System Analysis and Design: Conventional and Modern. New York: McGraw-Hill Book Company, 1965.
3. Golubitsky, Martin, "An Introduction to Catastrophe Theory and its Applications," Society for Industrial and Applied Mathematics Review, 20: 352-387 (April 1978).
4. Mehra, Raman K., W. C. Kessel, and J. V. Carroll, Global Stability and Control Analysis of Aircraft at High Angles-of-Attack, Arlington, Virginia: Technology Projects Division, Office of Naval Research, June 1977.
5. Roskam, Jan, Flight Dynamics of Rigid and Elastic Airplanes, Kansas: Roskam Aviation and Engineering Corporation, 1972.
6. Woodcock, R. J., T. P. Neal, T. M. Harris, F. E. Pritchard, C. R. Chalk, Military Specification - Flying Quantities of Piloted Airplanes, Wright-Patterson AFB, Ohio: Air Force Flight Dynamics Laboratory, August 1969.
7. Mehra, R. K. and Carroll, J. V. "Application of Bifurcation Analysis and Catastrophe Theory Methodology (BACTM) to Aircraft Stability Problems at High Angles-of-Attack," Proceedings of 1978 IEEE Decision and Control Conference: 186-192 (January 1979).
8. Gibson, John E. Nonlinear Automatic Control. New York: McGraw-Hill Book Company, 1963.
9. Woodcock, Alexander and Davis, Monte. Catastrophe Theory. New York: E. P. Dutton, 1978.

## APPENDIX A

### Development of Reduced Linearized Equation

The equations of linear motion and the equations of angular motion are:

$$\Sigma \Delta F_x = m(\dot{U} + WQ - VR) \quad (A-1)$$

$$\Sigma \Delta F_y = m(\dot{V} + UR - WP) \quad (A-2)$$

$$\Sigma \Delta F_z = m(\dot{W} + VP - UQ) \quad (A-3)$$

$$\Sigma \Delta L = \dot{P}I_x - \dot{R}J_{xz} + QR(I_z - I_y) - PQJ_{xz} \quad (A-4)$$

$$\Sigma \Delta M = \dot{Q}I_y + PR(I_x - I_z) + (P^2 - R^2)J_{xz} \quad (A-5)$$

$$\Sigma \Delta N = \dot{R}I_z - \dot{P}J_{xz} + PQ(I_y - I_x) + QRJ_{xz} \quad (A-6)$$

Assuming constant velocity (U) eliminates the X-force equation (A-1). Assuming constant roll rate ( $P_o$ ) eliminates the  $\Delta L$  moment equation (A-4). This assumption was made because the transient value of roll rate was not-needed for the stability analysis. Assuming  $V_o = W_o = Q_o = R_o = 0$ , then Equations A-2, A-3, A-5, and A-6 became

$$\Sigma \Delta F_y = m(\dot{v} + U_o r - wP_o) \quad (A-7)$$

$$\Sigma \Delta F_z = m(\dot{w} + vP_o - U_o q) \quad (A-8)$$

$$\Sigma \Delta M = \dot{q}I_y + P_o r(I_x - I_z) + (P_o^2 - r^2)J_{xz} \quad (A-9)$$

$$\Sigma \Delta N = \dot{r}I_z + P_o q(I_y - I_x) + qrJ_{xz} \quad (A-10)$$

where  $U_o$  and  $P_o$  are equilibrium values and  $v$ ,  $r$ ,  $w$ , and  $q$  are small perturbations from the equilibrium values.

Assuming that the aircraft has the XY plane as the plane of symmetry and selecting the X-axis as the symmetry axis, then  $J_{xz} = 0$ . Assuming  $\Sigma \Delta M = \Sigma \Delta N = \Sigma \Delta F_x = \Sigma \Delta F_z = 0$ , equations A-7 thru A-10 became

$$\Sigma \Delta M = \dot{q} I_y + P_o r (I_x - I_z) = 0 \quad (A-11)$$

$$\Sigma \Delta N = \dot{r} I_z + P_o q (I_y - I_x) = 0 \quad (A-12)$$

$$\Sigma \Delta F_y = \dot{\beta} + r - P_o \alpha = 0 \quad (A-13)$$

$$\Sigma \Delta F_z = \dot{\alpha} + P_o \beta - q = 0 \quad (A-14)$$

where  $\beta = v/U_o$  and  $\alpha = \Delta \alpha = w/U_o$ .

The aerodynamic moments, including all the stability derivatives for the m and n moment equations, are (Ref 1:21).

$$-C_{m_u} U - \frac{C}{2U_o} C_{m_{\dot{\alpha}}} \dot{\alpha} - C_{m_{\alpha}} \alpha - \frac{C}{2U_o} C_{m_q} \dot{\theta} \quad (A-15)$$

$$\frac{-J_{xz}}{S \bar{q} b} \dot{\phi} - \frac{b}{2U_o} C_{n_p} \dot{\phi} - \frac{b}{2U_o} C_{n_r} \dot{\psi} - C_{n_{\beta}} \beta \quad (A-16)$$

Equating equation A-11 and A-15 and letting  $\dot{q} = \dot{\theta}$  yields:

$$\frac{I_y}{S \bar{q} c} q - \frac{C}{2U_o} C_{m_q} q - \frac{C}{2U_o} C_{m_{\dot{\alpha}}} \dot{\alpha} - C_{m_{\alpha}} \alpha + \frac{I_x - I_z}{S \bar{q} c} P_o r = 0 \quad (A-17)$$

Equating equation A-12 and A-16 and letting  $\dot{r} = \dot{\psi}$  and  $P_o = \dot{\phi}$  yields:

$$\frac{I_z}{S \bar{q} b} \dot{r} - \frac{b}{2U_o} C_{n_r} \dot{r} - C_{n_{\beta}} \beta + \frac{(I_y - I_x)}{S \bar{q} b} = \frac{b}{2U_o} C_{n_p} P_o \quad (A-18)$$

Solving equations A-13 and A-14 for r and q yields:

$$r = P_o \alpha - \dot{\beta} \quad (\text{A-19})$$

$$q = P_o \beta + \dot{\alpha} \quad (\text{A-20})$$

and differentiating, results in

$$\dot{r} = P_o \dot{\alpha} - \ddot{\beta} \quad (\text{A-21})$$

$$\dot{q} = P_o \dot{\beta} + \ddot{\alpha} \quad (\text{A-22})$$

Substituting equations A-19 thru A-22 into equations A-17 and A-18 yields:

$$\begin{aligned} \frac{I_y}{S\bar{q}c} (P_o \dot{\beta} + \ddot{\alpha}) - \frac{c}{2U_o} C_{m_q} (P_o \beta + \dot{\alpha}) - \frac{c}{2U_o} C_{m_{\dot{\alpha}}} \dot{\alpha} - C_{m_{\alpha}} \alpha \\ + \frac{(I_x - I_z)}{S\bar{q}c} P_o (P_o \alpha - \dot{\beta}) = 0 \end{aligned} \quad (\text{A-23})$$

$$\begin{aligned} \frac{I_z}{S\bar{q}b} (P_o \dot{\alpha} - \ddot{\beta}) - \frac{b}{2U_o} C_{n_r} (P_o \alpha - \dot{\beta}) - C_{n_{\beta}} \beta + \frac{(I_y - I_x)}{S\bar{q}b} P_o (P_o \beta + \dot{\alpha}) \\ = \frac{b}{2U_o} C_{n_p} P_o \end{aligned} \quad (\text{A-24})$$

Regrouping and taking the Laplace transform of equations A-23 and A-24 yields:

$$\left[ \frac{(I_y - I_x + I_z)P_o}{S\bar{q}c} s - \frac{c}{2U_o} C_{m_q} P_o \right] \beta(s) + \left[ \frac{I_y}{S\bar{q}c} s^2 - \frac{c}{2U_o} (C_{m_q} + C_{m_\alpha^*}) s + \frac{(I_x - I_z)P_o^2}{S\bar{q}c} - C_{m_\alpha} \right] \alpha(s) = 0 \quad (A-25)$$

$$\left[ \frac{I_z}{S\bar{q}b} s^2 - \frac{b}{2U_o} C_{n_r} s - \frac{(I_y - I_x)P_o^2}{S\bar{q}b} + C_{n_\beta} \right] \beta(s) + \left[ \frac{-(I_z + I_y - I_x)P_o}{S\bar{q}b} s + \frac{b}{2U_o} C_{n_r} P_o \right] \alpha(s) = 0 \quad (A-26)$$

Equations A-25 and A-26 have the form

$$(a_1 s + a_0) \beta(s) + (b_2 s^2 + b_1 s + b_0) \alpha(s) = 0 \quad (A-27)$$

$$(c_2 s^2 + c_1 s + c_0) \beta(s) + (d_1 s + d_0) \alpha(s) = 0 \quad (A-28)$$

and the characteristic equation is fourth-order and is a function of  $P_o$ . The stability derivatives and aircraft dynamic terms are listed in the computer program EIGEN (Appendix E). When these values are substituted into equations A-25 and A-26, the characteristic equation becomes

$$s^4 + .382498s^3 + (1.6961P_o^2 + .11241)s^2 + (.403345P_o^2 + .017979)s + (.718984P_o^4 - .056358P_o^2 + .010219) = 0 \quad (A-29)$$

## APPENDIX B

### Development of Full Aircraft Linear Equations

The equations of linear motion and the equations of angular motion are:

$$\Sigma \Delta F_x = m(\dot{U} + WQ - VR) \quad (B-1)$$

$$\Sigma \Delta F_y = m(\dot{V} + UR - WP) \quad (B-2)$$

$$\Sigma \Delta F_z = m(\dot{W} + VP - UQ) \quad (B-3)$$

$$\Sigma \Delta L = \dot{P}I_x - \dot{R}J_{xz} + QR(I_z - I_y) - PQJ_{xz} \quad (B-4)$$

$$\Sigma \Delta M = \dot{Q}I_y + PR(I_x - I_z) + (P^2 - R^2)J_{xz} \quad (B-5)$$

$$\Sigma \Delta N = \dot{R}I_z - \dot{P}J_{xz} + PQ(I_y - I_x) + QRJ_{xz} \quad (B-6)$$

Let

$$\begin{aligned}
 U &= U_0, \quad u \approx 0 \\
 V &= V_0 + v, \quad V_0 = 0 \\
 W &= W_0 + w, \quad W_0 = U_0 \alpha_0 \\
 P &= P_0 + p, \quad P_0 = P_0 \\
 Q &= Q_0 + q, \quad Q_0 = 0 \\
 R &= R_0 + r, \quad R_0 = R_0
 \end{aligned}
 \quad (B-7)$$

The second-order terms have been ignored since the perturbations are small. The velocity (U) is assumed constant which eliminates the X-force equation B-1. After using Taylor series expansions of the nonlinear terms and substituting B-7, equations B-2 thru B-6 become

$$\Sigma \Delta F_y = m(U_o \dot{\beta} + U_o r - P_o U_o \alpha - U_o \alpha_o p) \quad (B-8)$$

$$\Sigma \Delta F_z = m(U_o \dot{\alpha} + P_o U_o \beta - U_o q) \quad (B-9)$$

$$\Sigma \Delta L = \dot{p} I_x - \dot{r} J_{xz} + q R_o (I_z - I_y) - q P_o J_{xz} \quad (B-10)$$

$$\Sigma \Delta M = \dot{q} I_y + r P_o (I_x - I_z) + p R_o (I_x - I_z) + (2P_o p - 2R_o r) J_{xz} \quad (B-11)$$

$$\Sigma \Delta N = \dot{r} I_z - \dot{p} J_{xz} + q P_o (I_y - I_x) + q R_o J_{xz} \quad (B-12)$$

where  $\alpha = \Delta \alpha \approx w/U_o$ ,  $\beta \approx v/U_o$ , and  $W_o \approx U_o \alpha_o$ .

Ignoring gravity and combining equations B-8 thru B-12 with their aerodynamic force and moment equations yields  
(Ref 5:4.113)

$$m U_o \dot{\beta} + m U_o r - m U_o P_o \alpha - m U_o \alpha_o p = \bar{q} s [C_{y_\beta} \beta + C_{y_p} \left(\frac{b}{2U_o}\right) p + C_{y_r} \left(\frac{b}{2U_o}\right) r + C_{y_{\delta_f}} \delta_f + C_{y_{\delta_r}} \delta_r] \quad (B-13)$$

$$m U_o \dot{\alpha} + m U_o P_o \beta - m U_o q = \bar{q} s [C_{z_\alpha} \alpha + C_{z_{\dot{\alpha}}} \dot{\alpha} + C_{z_q} \left(\frac{c}{2U_o}\right) q + C_{z_{\delta_s}} \delta_s] \quad (B-14)$$

$$\dot{q} I_y + [P_o (I_x - I_z) - 2R_o J_{xz}] r + [R_o (I_x - I_z) + 2P_o J_{xz}] p = \bar{q} s c [C_{m_\alpha} \alpha + C_{m_q} \left(\frac{c}{2U_o}\right) q + C_{m_{\dot{\alpha}}} \left(\frac{c}{2U_o}\right) \dot{\alpha} + C_{m_{\delta_s}} \delta_s] \quad (B-15)$$

$$\begin{aligned} \dot{p}I_x - \dot{r}J_{xz} + [R_o(I_z - I_y) - P_o J_{xz}]q = \bar{q}sb[C_{\ell_\beta} \beta \\ + C_{\ell_p} \left(\frac{b}{2U_o}\right) p + C_{\ell_r} \left(\frac{b}{2U_o}\right) r + C_{\ell_{\delta_f}} \delta_f + C_{\ell_{\delta_r}} \delta_r] \quad (B-16) \end{aligned}$$

$$\begin{aligned} \dot{r}I_z - \dot{p}J_{xz} + [P_o(I_y - I_x) + R_o J_{xz}]q = \bar{q}sb[C_{n_\beta} \beta \\ + C_{n_p} \left(\frac{b}{2U_o}\right) p + C_{n_r} \left(\frac{b}{2U_o}\right) r + C_{n_{\delta_f}} \delta_f + C_{n_{\delta_r}} \delta_r] \quad (B-17) \end{aligned}$$

The stability derivatives and aircraft dynamic terms are listed in the computer program EIGEN in Appendix E.

## APPENDIX C

### Development of Longitudinal and Lateral FCS

Differential equations were formed from each of the transfer functions in the longitudinal and lateral FCS. The physical variables  $X_1$  thru  $X_5$ ,  $Z_1$  thru  $Z_4$ ,  $\delta f$ ,  $\delta r$ , and  $\delta s$  are shown in figures 2.1 and 2.2.

#### Longitudinal FCS for $\alpha < 20.4$ Degrees

$$1) \quad X_1 = \left( \frac{10(57.3)}{S+10} \right) \alpha \quad (C-1)$$

yields the differential equation

$$\dot{X}_1 = 573\alpha - 10X_1 \quad (C-2)$$

$$2) \quad X_2 = \left( \frac{57.3 S}{S+1} \right) q \quad (C-3)$$

yields

$$\dot{X}_2 - 57.3\dot{q} = -X_2 \quad (C-4)$$

$$3) \quad X_3 = \frac{15Az}{32.2(S+15)} = \frac{15U_0(\dot{\alpha} - q)}{32.2(S+15)} \quad (C-5)$$

yields

$$\dot{X}_3 - \frac{15U_0}{32.2} \dot{\alpha} = \frac{-15U_0 q}{32.2} - 15X_3 \quad (C-6)$$

$$4) \quad X_4 = \frac{3S+15}{S+15} [0.161(X_1 + 0.7(F3)X_2) + (0.2X_2 - 0.5X_3)] \quad (C-7)$$

yields

$$-.161(3)\dot{X}_1 - 3[.161(F3)(.7) + .2]\dot{X}_2 + 3(.5)\dot{X}_3 + \dot{X}_4 = .161(15)X_1 + 15[.161(F3)(.7) + .2]X_2 - 15(.5)X_3 - 15X_4 \quad (C-8)$$

$$5) X_5 = F4 X_1 + 2.5(F3) X_4 + \frac{5}{S} (2.5)(F3)X_4 \quad (C-9)$$

yields

$$-F4\dot{X}_1 - 2.5(F3)\dot{X}_4 + \dot{X}_5 = 12.5(F3)X_4 \quad (C-10)$$

$$6) \delta_s = \left( \frac{20KS}{s+20} \right) X_5 \quad (C-11)$$

yields

$$\dot{\delta}_s = 20(KS)X_5 - 20\delta_s \quad (C-12)$$

#### Longitudinal FCS for $\alpha > 20.4$ Degrees

The differential equations for  $X_1$ ,  $X_2$ ,  $X_3$ , and  $\delta_s$  are the same.

$$7) X_4 = \left( \frac{3S+15}{S+15} \right) (.2X_2 - .5X_3) \quad (C-13)$$

yields

$$-.6\dot{X}_2 + 1.5\dot{X}_3 + \dot{X}_4 = 3X_2 - 7.5X_3 - 15X_4 \quad (C-14)$$

$$8) X_5 = F4X_1 + 2.5(F3)[X_4 + .5X_1 + .5(.7)(F3)X_2] + 2.5(F3)\left(\frac{5}{S}\right)[X_4 + .5X_1 + .5(.7)(F3)X_2] \quad (C-15)$$

yields

$$[-2.5(.5)(F3) - F4]\dot{X}_1 - 2.5(.5)(.7)(F3)^2\dot{X}_2 - 2.5(F3)\dot{X}_4 + \dot{X}_5 = 2.5(F3)(5)(.5)X_1 + 2.5(.5)(.7)(5)F3)^2X_2 + 2.5(F3)(5)X_4 \quad (C-16)$$

Lateral FCS

$$9) \delta_f = 57.3(.12) \left( \frac{20KF}{S+20} \right) p \quad (C-17)$$

yields

$$\dot{\delta}_f = 57.3(2.4)KFp - 20\delta_f \quad (C-18)$$

$$10) z_1 = \left( \frac{10}{57.3(S-10)} \right) p\alpha = \left( \frac{10}{57.3(S-10)} \right) [P_o\alpha + \alpha_o p] \quad (C-19)$$

yields

$$z_1 = \frac{10}{57.3} \alpha_o p + \frac{10}{57.3} P_o \alpha - 10z_1 \quad (C-20)$$

$$11) z_2 = \left( \frac{1.5S}{S+1} \right) (57.3r - z_1) \quad (C-21)$$

yields

$$-1.5(57.3)\dot{r} + 1.5\dot{z}_1 + z_2 = -z_2 \quad (C-22)$$

$$12) z_3 = \left( \frac{3S+15}{S+15} \right) z_2 \quad (C-23)$$

yields

$$-3\dot{z}_2 + \dot{z}_3 = 15z_2 - 15z_3 \quad (C-24)$$

$$13) z_4 = F8[z_3 + \text{GAIN1} \frac{.6}{32.2} A_y + .12(57.3) \left[ \frac{10}{S+10} (.0375 - .65(F7)) \right] p\alpha$$

$$= F8z_3 + \frac{F8(\text{GAIN1})(.6)U_o(\dot{\beta} + r)}{32.2} +$$

$$\frac{1.2(57.3)}{S+10} [.0375 - .65(F7)] (P_o\alpha + \alpha_o p) \quad (C-25)$$

yields

$$\frac{-10(F8)(GAIN1)(.6)(U_o) \dot{\beta}}{32.2} - \frac{F8(GAIN1)(.6)(U_o) \dot{r}}{32.2} - F8 \dot{z}_3$$

$$+\dot{z}_4 = 1.2(57.3)[.0375-.65(F7)]P_o \alpha + 1.2(57.3)[.0375-.65(F7)]\alpha_o p$$

$$\frac{+10(F8)(GAIN1)(.6)(U_o)}{32.2} r + 10(F8)z_3 - 10z_4 \quad (C-26)$$

$$14) \delta_r = \left( \frac{20KR}{S+20} \right) z_4 \quad (C-27)$$

yields

$$\dot{\delta}_r = 20(KR)z_4 - 20\delta_r \quad (C-28)$$

APPENDIX D

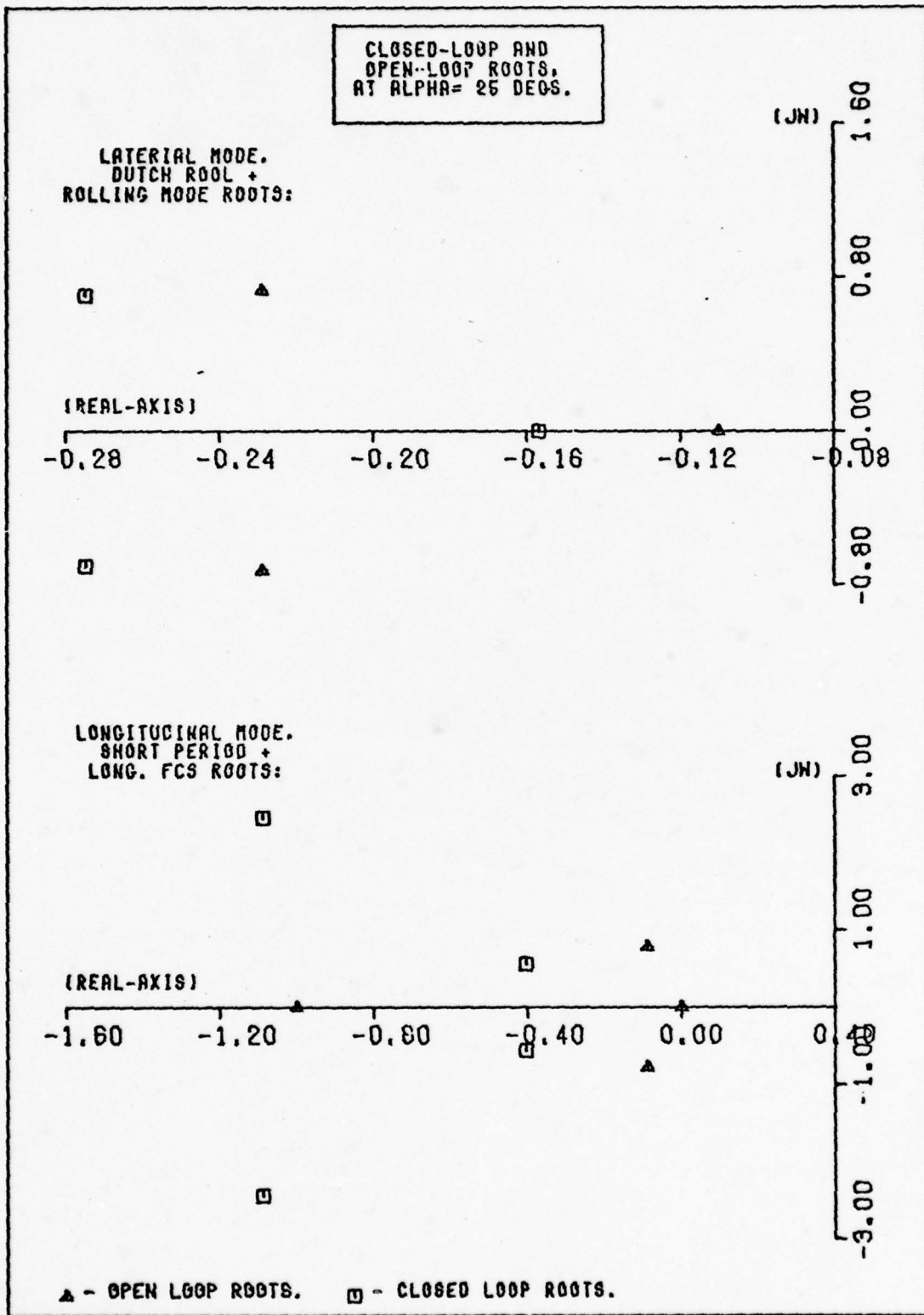


Fig. D.1 Closed Loop and Open Loop Roots for Aircraft

## APPENDIX E

- E1 - YFROOT -- Solves roots for equation 2.8.
- E2 - EIGEN -- Solves eigenvalues of full linearized model.
- E3 - RSVP -- Plotting program.
- E4 - NONLIN -- Solves equation 3.1.

E1

```
PROGRAM YFROOT (INPUT=780,OUTPUT,TAPE5=INPUT)
DIMENSION A(5),7(4)
REAL G1,G2,B1,B2,B3,C1,C2,D1,D2,D3
COMPLEX Z
```

\*\*\*\*\*  
\*\*\*\*\*  
C INPUTS TO PROGRAM:

```
C      U          - VELOCITY          - FT/SEC
C      IX,IY,IZZ  - MOMENTS OF INERTIA - SLUG-(FT**2)
C      JXZ        - PRODUCT OF INERTIA - SLUG-(FT**2)
C      P          - ROLL RATE         - RAD/SEC
C      PMAX       - MAXIMUM ROLL RATE - RAD/SEC
C      S          - SURFACE AREA      - FT**2
C      RE         - WING SPAN         - FT
C      CE         - CHORD             - FT
C      RHO        - AIR PRESSURE      - SLUGS/(FT**3)
C      MAS        - MASS              - SLUGS
```

C STABILITY DERIVATIVES:

```
C      CNR        - /RAD
C      CNB        - /5*DEG
C      CMQ        - /RAD
C      CMA        - /DEG
C      CMAD       - /DEG
```

```
*****
*****
NDEG=4
P=1.24
PMAX=1.23
U=425.0 IZZ=58600.0 IY=50000.0 IX=8200.0 JXZ=240.0
ALFA=0.5 S=283.0 BE=29.0 CE=10.94 SPDN=.000737 PC=497.45
MAS=134.0
CNR=-.53 CNB=.0105 CMQ=-4.4
CMAD=0.0 CMA=.0009
CMA=CMA+57.3
CNB=CNB+77.3/5
10  CRAR=.5*RON*(U**2)
15  G1=(IZZ+IY-IX)*P/(S*CRAR+BE)
    G2=-FE*CNR*P/(U**2)
    P1=IZZ/(S*CRAR+BE)
```

```

P2=-FE+CMR/(U*2)
P3=CMR-(IY-IX)*(P**2)/(S*OBAR*BE)
C1=(IY-IX+IZZ)*P/(S*OBAR*CE)
C2=-CE+CMQ*P/(U*2)
D1=IY/(S*OBAR*CE)
D2=-(E*(CMQ+CMAD))/(U*2)
D3=(IX-IZZ)*(P**2)/(S*OBAR*CE)-CM1
A(1)=1.0
A(2)=(P1*D2+P2*D1)/(P1*D1)
A(3)=(C1*G1+B1*D3+P2*D2+B3*D1)/(P1*D1)
A(4)=(C1*G2+C2*G1+P2*D3+P3*D2)/(P1*D1)
A(5)=(C2*G2+B3*D3)/(P1*D1)
CALL ZPOLR(A,NDEG,7,IFP)
IF(P.EQ.0) GO TO 20
PRINT*," "
PRINT*," "
PRINT*," "
PRINT*," "
PRINT*," "
PRINT*," "
GO TO 30
20 PRINT 100
30 PRINT*,"THE ROOTS ARE FOR P=","P," RAD/SEC"
PRINT*," "
PRINT*," "
DO 40 I=1,NDEG
PRINT*,7(I)
40 CONTINUE
P=P+.002
IF(P.LE.PMAX) GO TO 15
100 FORMAT(141)
END

```

```

PROGRAM EIGEN(INPUT=780,OUTPUT,TAPE5=INPUT)
DIMENSION A(17,17),W(17),Z(17,17),WK(40),B(17,17)
DIMENSION AINV(17,17),WKAREA(400),C(17,17)
DIMENSION P1(102),R1(102)
COMPLEX Z,W,ZN
REAL F3,F4,FA,E1,E2,E3,E4
REAL KF,KR,KS,F5,E6,F7

```

```

*****
*****

```

```

C THIS PROGRAM IS SET UP TO DO A LINEAR ANALYSIS, IN BODY
C AXIS, ON A PARTICULAR AIRCRAFT WITH A LONGITUDINAL AND
C LATERAL FCS. IT CAN SOLVE FOR BOTH EIGENVALUES AND EIGENVECTORS.
C TMSL SUBROUTINES ARE USED FOR THE ANALYSIS.

```

```

C OF THE 17 STATES, THE FIRST 5 ARE AIRCRAFT STATES:

```

```

C   BETA - SIDESLIP ANGLE - (RADIAN)
C   ALPHA - ANGLE OF ATTACK - (RADIAN)
C   Q - PITCH RATE - (RADIAN/SEC.)
C   P - ROLL RATE - (RADIAN/SEC.)
C   R - YAW RATE - (RADIAN/SEC.)

```

```

C THE FOLLOWING 6 STATES ARE FOR THE LONG. FCS

```

```

C   X1 - PHYSICAL VARIABLE
C   X2 - PHYSICAL VARIABLE
C   X3 - PHYSICAL VARIABLE
C   X4 - PHYSICAL VARIABLE
C   X5 - PHYSICAL VARIABLE
C   DELTA-S - STABILIZER ANGLE - (RAD.)

```

```

C THE LAST 6 STATES ARE FOR THE LAT. FCS

```

```

C   DELTA-F - FLAPERON ANGLE - (RAD.)
C   Z1 - PHYSICAL VARIABLE
C   Z2 - PHYSICAL VARIABLE
C   Z3 - PHYSICAL VARIABLE
C   Z4 - PHYSICAL VARIABLE
C   DELTA-R - RUDDER ANGLE - (RAD.)

```

```

*****
*****

```

C INPUTS TO PROGRAM:

C U - VELOCITY - FT/SEC  
 C ALT - ALTITUDE - FT  
 C IX,IY,IZ - MOMENTS OF INERTIA - SLUG-(FT\*\*2)  
 C JX7 - PRODUCT OF INERTIA - SLUG-(FT\*\*2)  
 C ALFA - ANGLE OF ATTACK - DEGREES  
 C P - ROLL RATE - RAD/SEC  
 C PMAX - MAXIMUM ROLL RATE - RAD/SEC  
 C R - YAW RATE - RAD/SEC  
 C S - SURFACE AREA - FT\*\*2  
 C CE - CHORD - FT  
 C RE - WING SPAN - FT  
 C POW - AIR PRESSURE - SLUGS/(FT\*\*3)  
 C PC - STATIC PRESSURE - LBS/(FT\*\*2)  
 C MAS - MASS - SLUGS

C STABILITY DERIVATIVES:

C CNF - /RAD CYR - /RAD  
 C CNB - /5\*DEG CYB - /DEG  
 C CNP - /RAD CYP - /RAD  
 C CNDF - /DEG CYDF - /DEG  
 C CNDR - /DEG CYDR - /DEG  
 C CLR - /RAD CZA - /RAD  
 C CLB - /5\*DEG CZAD - /RAD  
 C CLF - /RAD CZO - /RAD  
 C CLDF - /DEG CZDS - /RAD  
 C CLDR - /DEG CMA - /DEG  
 C CMC - /RAD CMAO - /DEG  
 C CMDS - /DEG

C F3,F4,F7,F8 - FDS PARAMETERS, SOLVED FOR IN PROGRAM.

C KF,KF,KS,  
 C GAIN1,GAIN2 - DUMMY PARAMETERS USED TO ANALYSE CERTAIN  
 C FEEDBACK LOOPS, USUALLY SET TO 1.

\*\*\*\*\*  
 C The program runs for the last value of alfa read. Interchange  
 C cards to run for different values of alfa.

ALFA=0.  
 ALFA=10.  
 POW=.00233PC=21169ALT=0.  
 U=425.3I77=52600.3IY=50000.3IX=5200.3JX7=240.3ALT=35000.  
 ALFA=20.3S=287.3CE=10.340RF=29.3RD4=.0007375PC=497.95  
 ALFA=25.

MAS=134.

ALPHA=ALFA

1 IF(ALFA.EQ.0) GO TO 2

IF(ALFA.EQ.10) GO TO 3

IF(ALFA.EQ.25) GO TO 4

CNR=-.50733CNR=.013040=-4.52910MAJ=.299

CMA=.00433CLPF=.000523CNDP=-.00013CLDR=.00052

CNDR=-.001353CNP=.00483CLP=-.18373CLP=-.005

CLR=.27443CYR=-.01843CYDF=.000073CYDR=.00305

CZA=-3.43807AD=-1.51773CZD=-3.23530ZDS=-.5767

CMDS=-.00733CYP=0.3CYP=0.

GO TO 5

2 CNR=-.53503CNR=.01053040=-4.43040MAJ=0.

CMA=.00033CLPF=.001353CNDP=.00023CLDR=.00057

CNDR=-.00143CNP=0.3CLP=-.273CLP=-.0046

CLR=.12833CYR=-.02363CYDF=-.000233CYDR=.00334

CZA=-3.9307AD=-1.0033070=-2.00700ZDS=-.573

CMDS=-.01303CYP=0.3CYP=0.

GO TO 5

3 CNR=-.50133013=.0133040=-4.78053040=.1805

CMA=.00633CLPF=.001103CNDP=.000533CLDR=.00055

CNDR=-.001733CNP=.0113CLP=-.25873CLP=-.0077

CLR=.22733CYR=-.02233CYDF=-.000133CYDR=.00325

CZA=-3.05693CZAD=-1.25563CZD=-2.51133CZDS=-.54

CMDS=-.01303CYP=0.3CYP=0.

GO TO 5

4 CNR=-.56893CNR=.00353040=.21493040=-.2149

CMA=-.00333CLPF=.000423CNDP=-.000143CLDR=.00049

CNDR=-.001563CNP=.10373CLP=-.12323CLP=-.0025

CLR=.23173CYR=-.01433CYDF=-.000053CYDR=.00283

CZA=-2.9723CZAD=-2.12973CZD=-4.25333CZDS=-.673

CMDS=-.00733CYP=0.3CYP=0.

IDGT=0

\*\*\* NOW CONVERT STAB. DERIV. TO DESIRED UNITS.

CZDS=CZDS/57.3

CNR=(CNR\*57.3/5)

CLR=(CLR\*57.3/5)

CYR=(CYR\*57.3)

CMA=(CMA\*57.3)

\*\*\* IJOB=0. FOR EIGENVALUES ONLY.

\*\*\* IJOB=1. FOR EIGENVALUES AND EIGENVECTORS.

IJOB=1

IJOB=0

P=0

PMAX=12.

R=C

I1=1

```

K=17
L=17
M=17
N=17
IA=17
IB=17
IC=17
IZ=17
KF=-1.
KR=1.
KS=1.
GAIN1=1.
GAIN2=1.
ALFA=ALFA/37.3
QBAR=.5*RDW*(U**2)
RATIO=QBAR/PC

```

\*\*\* CALCULATIONS FOR FCS PARAMETERS.

```

F1=(-.64*(QBAR-100)/500+.64)+.35
F2=(-.224*(QBAR-100)/2200+.224)+.175
F3=.5*(RATIO-2.04)/1.10+.5
F4=(-1.5*(RATIO-.53)/1.26+1.5)-1.0
F5=1.0016*RATIO-.1935
F6=-.6575*RATIO+2.1236
IF(QBAR.LT.100) F3=1.0
IF(QBAR.GE.150) F3=F1
IF(QBAR.GE.800) F3=F2
IF(QBAR.GE.3000) F3=.136
IF(RATIO.LT..53) F4=.5
IF(RATIO.GE..53) F4=F4
IF(RATIO.GE.1.73) F4=-1.0
IF(RATIO.LT.0.187) F7=0.
IF(RATIO.GE.0.187) F7=F5
IF(RATIO.GE.1.125) F7=1.
IF(RATIO.GE.1.709) F7=F6
IF(RATIO.GE.3.23) F7=0.
IF(RATIO.LT.2.04) F8=.7
IF(RATIO.GE.2.04) F8=F7
IF(RATIO.GE.3.23) F8=1.0

```

```

*****
*
* SET UP STATE MATRIX (A)*XDOT=(R)*X
* AND SOLVE FOR EIGENVALUES OF (A-INVERSE)*B
*
*
*****

```

```

DO 15 I=1,N
DO 15 J=1,N
A(I,J)=0
R(J,J)=0
17 CONTINUE
A(1,1)=MAS*U
A(2,2)=MAS*U-QBAR*S*Q7AD
A(3,2)=-QBAR*S*(CE**2)*CMAD/(2*U)
A(3,3)=IY
A(4,4)=IX
A(4,5)=-JXZ
A(5,4)=-JXZ
A(5,5)=I7Z
DO 21 I=3,4
A(I,I)=1
27 CONTINUE
A(7,3)=-57.3
A(8,2)=-U*18/32.2
A(9,6)=-.433
A(9,7)=(.151+.7*F3+.2)*(-3)
A(9,8)=1.5
A(10,6)=-F4
A(10,9)=-2.5*F3
A(14,5)=-1.5*57.3
A(14,13)=1.5
A(15,14)=-3
A(16,1)=-11*F8*GAIN1*.6*U/32.2
A(16,5)=-F8*GAIN1*.5*U/32.2
A(16,15)=-F8
B(1,1)=QBAR*S*CYB
B(1,2)=MAS*U*P
B(1,4)=MAS*U*ALFA+QBAR*S*BE*CYB/(2*U)
B(1,5)=-MAS*U+QBAR*S*BE*CYB/(2*U)
B(1,12)=QBAR*S*CYDE
B(1,10)=QB1F*S*CY7R
B(2,1)=-MAS*U*P
B(2,2)=QBAR*S*Q7A
B(2,3)=MAS*U+QBAR*S*CE*Q7O/(2*U)
B(2,11)=QBAR*S*Q7DS
B(3,2)=QBAR*S*CE*Q7A
B(3,7)=QBAR*S*(CE**2)*CMQ/(2*U)
B(3,4)=-P*(IX-I7Z)-2*JXZ*P
B(3,5)=2*P-JXZ-P*(IX-I7Z)
B(3,11)=QBAR*S*CE*Q7DS
B(4,1)=QBAR*S*3F*CL3
B(4,7)=P-JXZ-P*(I7Z-IY)
B(4,4)=QB1F*S*(3E**2)*CLP/(2*U)
B(4,5)=QBAR*S*(3E**2)*CLR/(2*U)
B(4,12)=QBAR*S*3E*CLDE
B(4,16)=QB1F*S*3E*CLDE
B(5,1)=QBAR*S*BE*Q7N3

```

```

B(5,3)=-P*(IY-IX)-R'JX7
B(5,4)=QBAR*S*(3E**2)+CNP/(2*U)
B(5,5)=QBAR*S*(3E**2)*CNR/(2*U)
B(5,12)=QBAR*S*3E*CNDP
B(5,16)=QBAR-S*3E*CNDP
B(6,2)=10*57.3
B(6,6)=-10
B(7,7)=-1
B(8,3)=-U*15/32.2
B(8,8)=-15
B(9,6)=2.415
B(9,7)=(.161-.7**F3+.2)*15
B(9,8)=-7.5
B(9,9)=-15
B(10,9)=12.5*F3
B(11,10)=20*KS
B(11,11)=-20
B(12,4)=17.3*2.4*KF
B(12,12)=-20
B(13,2)=573**2
B(13,4)=10*57.3*ALFA
B(13,13)=-10
B(14,14)=-1
B(15,14)=15
B(15,15)=-15
B(16,2)=1.2*57.3*(.137**-.6**F7)**2
B(16,4)=1.2*57.3*(.137**-.6**F7)*ALFA
B(16,5)=10*F8*GAIN1*.6*U/32.2
B(16,15)=10*F8
B(16,16)=-10
B(17,16)=20*KR
B(17,17)=-20
IF(ALFA.LE.20.4) GO TO 26
A(9,6)=0.
A(9,7)=-.5
A(10,6)=-2.5*.5*F3=F4
A(10,7)=-2.5*.5*.7*(F3**2)
A(9,6)=0.
A(9,7)=3.
B(10,6)=2.5*.5*F3=F4
B(10,7)=2.5*.5*.7*F3*(F3**2)
23 CALL LINV1F(A,N,IA,AINV,IOGT,WKAREA,IER)
DO 30 I=1,N
DO 30 J=1,N
A(I,J)=AINV(I,J)
30 CONTINUE
CALL VMULF(A,B,L,M,N,TA,IB,OC,IC,IER)
DO 32 I=1,N
DO 32 J=1,N
A(I,J)=C(I,J)
77 CONTINUE

```

```

CALL EIGRF(A,N,IF,1JOB,W,Z,IZ,WV,IER)
IF(P.EQ.J) GO TO 35
PRINT*," "
PRINT*," "
PRINT*," "
PRINT*," "
GO TO 45
35 PRINT 100
PRINT*,"***** DROP MODEL *****"
PRINT*," "
PRINT*," "
PRINT*," "
PRINT*,"FOR VELOCITY, U=","U," FT./SEC."
PRINT*," "
PRINT*,"AT AN ALTITUDE OF " ,ALT," FT."
PRINT*," "
PRINT*,"AND AN ANGLE OF ATTACK OF " ,ALPHA," DEGREES"
PRINT*," "
PRINT*," "
PRINT*,"FEEDBACK PARAMETERS:"
PRINT*," "
PRINT*," F3=" ,F3
PRINT*," F4=" ,F4
PRINT*," F5=" ,F5
PRINT*," "
PRINT*," "
PRINT*," "
47 PRINT*,"THE EIGENVALUES ARE:"
PRINT*," "
PRINT*,"FOR ROLL RATE, P=" ,P," RAD/SEC"
PRINT*,"AND FOR YAW RATE, R=" ,R," RAD/SEC"
PRINT*," "
PRINT*," "
DO 55 I=1,N
PRINT* ,W(I)
55 CONTINUE
IF(1JOB.EQ.0) GO TO 70
PRINT*," "
PRINT*," "
PRINT*," "
PRINT*,"THE CORRESPONDING EIGENVECTORS ARE:"
PRINT*," "
PRINT*," "
JJ=1
61 JJJ=JJ+3
DO 62 I=1,N
WRITE 200,(7(I,J),J=JJ,JJJ)
62 CONTINUE
PRINT*," "
PRINT*," "
JJ=JJJ+1

```

```
IF (JJ.LT.N) GO TO 61
DO 64 I=1,N
WRITE 22),7 (I,N)
50 CONTINUE
KS=1-KS
KR=1-KR
KF=1+KF
IF (KF.EQ.0) GO TO 6
GO TO 300
70 F=P+.2
R=F*TAN(ALFA)
IF (P.LE.PMAX) GO TO 5
100 FORMAT (1H1)
200 FORMAT (1X,+(1H(,G12.6,2H, ,E12.6,1H),5X))
220 FORMAT (1X,1H (,G12.6,2H, ,E12.6,1H))
300 STOP
END
```

E3

```
PROGRAM RVSP(INPUT,OUTPUT,TAPE7)
DIMENSION A(52),B(52),C(52),D(52),E(52),F(52),G(52),H(52)
DIMENSION P1(52),P2(52),P3(52),P4(52),R1(52),R2(52),R3(52),R4(52)
DIMENSION AA(104),BB(104),CC(104),DD(104)
DIMENSION EE(104),FF(104),GG(104),HH(104)
DATA N,XLEN,YLEN/50,2.5,2.5/
DATA V,V1,V2,V3/7.,1.4,4.0,4.8/
DATA AL1,AL2,AL3,AL4/0.,10.,20.,25./
DATA A/50*1./
AL1=AL1/57.3
AL2=AL2/57.3
AL3=AL3/57.3
AL4=AL4/57.3
B(1)=0.
C(1)=2.
E(1)=2.4
G(1)=2.2
P1(1)=0.
P2(1)=0.
P3(1)=0.
P4(1)=0.
DO 10 J=1,N
B(I+1)=B(I)+V/50
C(I+1)=C(I)+V1/50
D(I)=7.*C(I)/1.4-10
E(I+1)=E(I)+V2/50
IF(E(I).LE.4.4) F(I)=3*(E(I)-2.4)/2
IF(E(I).GT.4.4) F(I)=E(I)-1.4
IF(E(I).GT.8.4) F(I)=5.
G(I+1)=G(I)+V3/50
IF(G(I).LT.3.4) H(I)=G(I)/1.2-2.2/1.2
IF(G(I).GE.3.4) H(I)=1.
P1(I+1)=P1(I)+7./50
P1(I)=P1(I)*TAN(AL1)
P2(I+1)=P2(I)+7./50
P2(I)=P2(I)*TAN(AL2)
P3(I+1)=P3(I)+7./50
P3(I)=P3(I)*TAN(AL3)
P4(I+1)=P4(I)+7./50
P4(I)=P4(I)*TAN(AL4)
1* CONTINUE
DO 20 I=1,N
AA(I)=A(I)
AA(I+50)=P1(I)
BB(I)=B(I)
BB(I+50)=R1(I)
CC(I)=C(I)
CC(I+50)=P2(I)
DD(I)=D(I)
DD(I+50)=P3(I)
EE(I)=E(I)
```

```

FE(I+50)=P3(I)
FF(I)=F(I)
FF(I+50)=R3(I)
GG(I)=G(I)
GG(I+50)=P4(I)
HH(I)=H(I)
HH(I+50)=R4(I)
20 CONTINUE
CALL PLOT(2.,-2.,-3)
CALL PLOT(3.,1.5,-3)
CALL PLOT(0.,8.5,-2)
CALL PLOT(6.25,0.,-2)
CALL PLOT(0.,-8.5,-2)
CALL PLOT(-6.25,0.,-2)
CALL SYMBOL(2.31,8.375,.08,21BODY VS VELOCITY AXIS,0.,21)
CALL SYMBOL(2.59,8.25,.08,22H- LINES OF INSTABILITY,0.,22)
CALL SYMBOL(2.331,8.125,.08,30H- LINES FOR VELOCITY AXIS ROLL,0.,3
+0)
CALL SYMBOL(1.820,8.1645,.0833,11,0.,-1)
CALL SYMBOL(2.191,8.1645,.0833,11,0.,-1)
CALL SYMBOL(2.375,8.0,.08,19AOA=ANGLE OF ATTACK,0.,19)
CALL PLOT(1.984,8.239,-3)
CALL PLOT(.5,0.,-2)
CALL PLOT(-.693,-.125,-3)
CALL PLOT(.5,0.,-2)
CALL PLOT(-2.260,-8.164,-3)
CALL PLOT(.625,.75,-3)
CALL SCALE(EE,XLEN,100,1)
CALL SCALE(FF,YLEN,100,1)
E(N+1)=EE(101)
E(N+2)=EE(102)
P3(N+1)=EE(101)
P3(N+2)=EE(102)
F(N+1)=FF(101)
F(N+2)=FF(102)
R3(N+1)=FF(101)
R3(N+2)=FF(102)
CALL AXIS(0.,0.,10HP(RAD/SEC),-10,YLEN,0.,EE(101),EE(102))
CALL AXIS(0.,0.,10HR(RAD/SEC),10,YLEN,90.,FF(101),FF(102))
CALL SYMBOL(.125,2.5,.08,12H20 DEG. AOA,0.,12)
CALL LINE(E,F,N,1,0,0)
CALL LINE(P3,R3,N,1,10,11)
CALL PLOT(0.,4.,-3)
CALL SCALE(AA,XLEN,100,1)
CALL SCALE(BB,YLEN,100,1)
A(N+1)=A1(101)
A(N+2)=A4(102)
P1(N+1)=AA(101)
P1(N+2)=AA(102)
R(N+1)=BB(101)
R(N+2)=BB(102)

```

```

P1(N+1)=R1(101)
P1(N+2)=R1(102)
CALL AXIS(0.,0.,10HR(RAD/SEC),-10,XLEN,0.,AA(101),AA(102))
CALL AXIS(0.,0.,10HR(RAD/SEC),10,YLEN,90.,BB(101),BR(102))
CALL SYMBOL(.125,2.5,.08,12H 0 DEG. AOA:,0.,12)
CALL LINE(A,E,N,1,0,0)
CALL LINE(P1,R1,N,1,10,11)
CALL PLOT(3.,0.,-3)
CALL SCALE(CC,XLEN,100,1)
CALL SCALE(DD,YLEN,100,1)
C(N+1)=CC(101)
C(N+2)=CC(102)
P2(N+1)=CC(101)
P2(N+2)=CC(102)
D(N+1)=DD(101)
D(N+2)=DD(102)
R2(N+1)=DD(101)
R2(N+2)=DD(102)
CALL AXIS(0.,0.,10HR(RAD/SEC),-10,XLEN,0.,CC(101),CC(102))
CALL AXIS(0.,0.,10HR(RAD/SEC),10,YLEN,90.,DD(101),DD(102))
CALL SYMBOL(.125,2.5,.08,12H10 DEG. AOA:,0.,12)
CALL LINE(C,J,N,1,0,0)
CALL LINE(P2,R2,N,1,10,11)
CALL PLOT(0.,-4.,-3)
CALL SCALE(GG,XLEN,100,1)
CALL SCALE(HH,YLEN,100,1)
G(N+1)=GG(101)
G(N+2)=GG(102)
P4(N+1)=GG(101)
P4(N+2)=GG(102)
H(N+1)=HH(101)
H(N+2)=HH(102)
R4(N+1)=HH(101)
R4(N+2)=HH(102)
CALL AXIS(0.,0.,10HR(RAD/SEC),-10,XLEN,0.,GG(101),GG(102))
CALL AXIS(0.,0.,10HR(RAD/SEC),10,YLEN,90.,HH(101),HH(102))
CALL SYMBOL(.125,2.5,.08,12H25 DEG. AOA:,0.,12)
CALL LINE(G,H,N,1,0,0)
CALL LINE(P4,R4,N,1,10,11)
CALL PLOT
END

```

```

PROGRAM NONLIN(INPUT,OUTPUT,TAPES=0)OUTPUT)
COMMON/CALFUN/C1,C2
DIMENSION X(2),F(2),AJTINV(2,2),H(100),P1(30,100),S(30,100)
DIMENSION AA(100),BB(100),CC(100),DD(100),EE(100)
DIMENSION FF(100),GG(100),HH(100),COUNT(30)
DIMENSION DX(1),XMAX(1),XMIN(1),INIT(30)
REAL INIT,R1
INTEGER Y,V,I1,J1,V1,V2,V3,V4

```

```

*****
*****

```

C INPUTS TO PROGRAM

```

C C1,C2 - STARTING VALUE OF CONTROL VARIABLES.
C I1,I2 - INTEGER COUNTS OF INCREMENTS OF C1 & C2.
C N - NUMBER OF EQUATIONS.
C Q,P - INCREMENTS OF C1 & C2, RESPECTIVELY.
C EFOR - THE + OR - VALUE TO ACCEPT FOR BIFURCATION POINT.
C INIT - THE INITIAL GUESS OF X FOR EACH INCREMENT OF C1.
C C1MAX,C2MAX - THE MAXIMUM VALUE OF C1 & C2.
C DSTEP - STEP LENGTH USED IN NS01A.
C MAXFUN - MAXIMUM NUMBER OF EXECUTIONS.
C DMAX - ESTIMATE OF DISTANCE TO SOLUTION.
C ACC - ACCURACY REQUIRED FOR SOLUTION.

```

```

*****
*****

```

```

DATA C1,C2,I1,J1,N,Q,P,DELTA/-3.,-3.,1,1,2,.5,.2,.001/
DATA INIT/1.8,1.7,1.6,1.5,1.4,1.3,1.2,1.1,1.,.01,0./
DATA C1MAX,C2MAX,X/3.0,3.,2.,2./
DATA DSTEP,MAXFUN,DMAX,ACC/.001,100,20.,.1E-10/
DATA EFOR/.05/

```

```
PRINT 100
```

```
PRINT*,"*****DATA FOR SINGLE NONLINEAR EQUATIONS*****"
```

```
PRINT*," "
```

```
PRINT*," "
```

```
PRINT*," "
```

```
CALL NS01A(N,X,F,AJTINV,DSTEP,DMAX,ACC,MAXFUN,Q,W)
```

```
R1(I1,J1)=X(1)
```

```
CALL PENT(X,F,EFOR,C1,C2,N)
```

```
IF(C1.GE.0.0) GO TO 10
```

```
CALL DERIV(X,C1,DELTA,YMAX,XMIN,R1,EFOR,DX,DIFF,P,I1,J1,XAR)
```

```
10 S(I1,J1)=C2
```

```
C2=C2+P
```

```
IF(CC.GT.C2MAX) GO TO 10
```

```

J1=J1+1
GO TO 4
30 C1=C1+D
C2=-3.
COUNT(I1)=J1
IF(C1.GT.C1MAX) GO TO 55
J1=1
I1=I1+1
X(1)=INIT(I1)
X(2)=INIT(I1)
GO TO 5
37 STOP
50 CALL PLOTT(R1,S,AA,33,CC,DD,EE,FF,GG,HH,COUNT,I,J)
100 FORMAT(1H1)
END

```

```

SUBROUTINE CALFUN(N,X,F)
COMMON/CALFUN/C1,C2
DIMENSION X(1),F(1)
F(1)=C2+(X(1)*X(1)+C1)*X(1)
F(2)=C2+(X(2)*X(2)+C1)*X(2)
RETURN
END

```

```

SUBROUTINE PENT(Y,F,FSC,C1,C2,N)
DIMENSION X(1),F(1)
INTEGER Y,V
FSQ=0
DO 1 Y=1,N
FSQ=FSQ+F(Y)*F(Y)
1 CONTINUE
PRINT*," "
PRINT*," "
PRINT*," "
PRINT*," "
PRINT*,"FOR C1=",C1," & C2=",C2
PRINT 200,(Y,X(Y),F(Y),Y=1,N)
PRINT 210,FSQ
200 FORMAT(//4X,"Y",1X,"X(Y)",12X,"F(Y)"/(I5,2E17.8))
210 FORMAT(/5X,"THE SUM OF SQUARES IS",E17.8)
RETURN
END

```

```

SUBROUTINE DERIV(X,C1,DELTA,XMAX,XMIN,P1,EPOR,DX,DIFF,P,I,J,YAR)
DIMENSION Y(2),XMAX(1),XMIN(1),I(30,100),DX(1)
DX(1)=(-C1/3)**.5
XMAX(1)=DX(1)+EROR
XMIN(1)=DX(1)-EROR
YAR=ABS(Y(1))
IF(XAR.LE.XMIN.OR.YAR.GE.XMAX) RETURN
DIFF=R1(I,J)-R1(I,J-1)
X(1)=X(1)+DIFF-.1*DIFF
X(2)=X(1)
P=-P
RETURN
END

```

```

SUBROUTINE PLOTT(R1,S,AA,BB,CC,DD,EE,FF,GG,HH,COUNT,I,J)
DIMENSION R1(30,100),S(30,100),AA(100),BB(100),CC(100)
DIMENSION DD(100),EE(100),FF(100),GG(100),HH(100),COUNT(30)
INTEGER V1,V2,V3,V4
XLEN=2.5
YLEN=2.5
V1=COUNT(1)
V2=COUNT(5)
V3=COUNT(9)
V4=COUNT(13)
DO 300 J=1,V1
AA(J)=F1(1,J)
BB(J)=S(1,J)
300 CONTINUE
DO 310 J=1,V2
CC(J)=R1(5,J)
DD(J)=S(5,J)
310 CONTINUE
DO 320 J=1,V3
EE(J)=R1(9,J)
FF(J)=S(9,J)
320 CONTINUE
DO 330 J=1,V4
GG(J)=R1(13,J)
HH(J)=S(13,J)
330 CONTINUE
CALL PLOT(2.,-2.,-3)
CALL PLOT(0.,2.,-3)
CALL PLOT(-.5,-.75,-3)
CALL PLOT(0.,6.75,-2)
CALL PLOT(6.25,0.,-2)
CALL PLOT(0.,-3.75,-2)
CALL PLOT(-6.25,0.,-2)
CALL PLOT(.375,.75,-3)
CALL SYMBOL(2.052,7.212,.08,18HXDOT= X3+C1·X+C2,0.,18)
CALL SYMBOL(2.122,7.562,.08,19H- BIFURCATION POINT,0.,19)
CALL SYMBOL(1.935F,7.476,.08,11.0.,-1)
CALL SYMBOL(.0625,2.5,.1562,14X,0.,1)
CALL SYMBOL(.0625,7.,.1562,14X,0.,1)
CALL SYMBOL(3.0625,7.,.1562,14X,0.,1)
CALL SYMBOL(3.0625,2.5,.1562,14X,0.,1)

CALL SCALE(FF,XLEN,V3,1)
CALL SCALE(EE,YLEN,V3,1)
CALL AXIS(0.,0.,1140?--(C1=1.),-11,XLEN,0.,FF(V3+1),FF(V3+2))
CALL AXIS(0.,0.,14,1,YLEN,90.,EE(V3+1),EE(V3+2))
CALL LINE(FF,EE,V3,1,0,0)
CALL PLOT(0.,4.5,-3)

CALL SCALE(BB,XLEN,V1,1)
CALL SCALE(AA,YLEN,V1,1)

```

```

CALL AXIS(0.,0.,12HC2--(C1=-3.),-12,XLEN,0.,BB(V1+1),BB(V1+2))
CALL AXIS(0.,0.,14,1,YLEN,90.,AA(V1+1),AA(V1+2))
CALL SYMBOL(1.5,1.25,.08,11,0.,-1)
CALL SYMBOL(.5,.75,.08,11,0.,-1)
CALL SYMBOL(1.25,.75,.08,SHUNSTAR_F,0.,8)
CALL ARCHD(1.125,.82,.9375,.9625,.03,.08,15)
CALL LINE(BB,AA,V1,1,0,0)
CALL PLOT(3.,0.,-3)

```

```

CALL SCALE(CC,YLEN,V2,1)
CALL SCALE(CC,YLEN,V2,1)
CALL AXIS(0.,0.,12HC2--(C1=-1.),-12,XLEN,0.,DD(V2+1),DD(V2+2))
CALL AXIS(0.,0.,14,1,YLEN,90.,CC(V2+1),CC(V2+2))
CALL SYMBOL(1.034,1.312,.08,11,0.,-1)
CALL SYMBOL(.905,.586,.08,11,0.,-1)
CALL SYMBOL(1.375,.75,.08,SHUNSTABLE,0.,8)
CALL ARCHD(1.25,.82,1.,1.,.08,.03,15)
CALL LINE(DD,CC,V2,1,0,0)
CALL PLOT(0.,-4.5,-3)

```

```

CALL SCALE(HH,XLEN,V4,1)
CALL SCALE(GG,YLEN,V4,1)
CALL AXIS(0.,0.,11HC2--(C1=3.),-11,XLEN,0.,HH(V4+1),HH(V4+2))
CALL AXIS(0.,0.,14,1,YLEN,90.,GG(V4+1),GG(V4+2))
CALL LINE(HH,GG,V4,1,0,0)
CALL PLOT
RETURN
END

```

## APPENDIX F

### Explanations of Program

#### YFROOT

This program is set up to solve the polynomial equation which was derived in the reduced linearized model analysis. It uses the IMSL subroutine ZPOLR which solves for the roots of a polynomial equation. The accuracy of ZPOLR was checked by setting  $P = 0$  and solving for the roots of the polynomial using the computer program TOTAL. YFROOT had an accuracy of at least  $10^{-3}$  which was considered sufficient. ZPOLR was set up to solve for the roots repetitively while incrementing the roll rate. The inputs are specified in the program YFROOT in Appendix E. No programming problems were encountered.

#### EIGEN

This program is, for the most part, self explanatory. It is limited to angles of attack of 0, 10, 20, and 25 degrees and to two altitudes: 0 and 35,000 ft. Different altitudes can be used if the correct values of ROW, PC, and ALT are fed into the program. EIGEN uses the following IMSL subroutines: LINVIF, which inverts a matrix; VMULFF, which multiplies two matrices together; and ElGRF, which solves for the eigenvalues and eigenvectors of a matrix. Several test cases were run with simple  $2 \times 2$  matrices for which the results were known. This was done to verify that these subroutines did work. There were no programming problems except for making sure that the work areas for the subroutines were dimensioned properly.

AD-A069 301

AIR FORCE INST OF TECH WRIGHT-PATTERSON AFB OHIO SCH--ETC F/G 1/3  
INVESTIGATION OF ROLL PERFORMANCE FOR A HIGHLY NONLINEAR STATIC--ETC(U)  
MAR 79 P L VERGEZ

UNCLASSIFIED

AFIT/G6C/EE/79-4

NL

2 OF 2

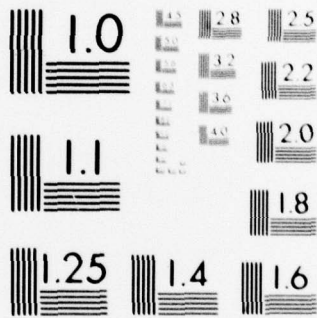
AD  
A069301



END  
DATE  
FILMED

7-79

DDC



MICROCOPY RESOLUTION TEST CHART  
NATIONAL BUREAU OF STANDARDS 1963-A

### RSVP

This program is set up to plot four graphs, each with two arrays, on the ASD Calcomp Plotter. The inputs are equations which cannot be changed. All the plotting programs presented the biggest programming problems. Dimensioning is most important; the array must allow for all the data points plus two extra spaces needed for the Calcomp Plotter routines. The largest problem arose when trying to scale one axis for more than one curve. To get around it, there must be one array which contains all the curves needed on one plot. This one array is used for scaling. Then, before calling the routine LINE to plot these curves, the adjusted minimum and adjusted delta, that was obtained from scaling the larger array, must be set as the adjusted minimum and adjusted delta for each of the curves to be plotted.

It is very important to know where the pen of the plotter is at all times. The "ASD Computer Center Calcomp Plotter Guide" is a useful aid for developing plotting programs.

### NONLIN

This program is set up to solve for two identical decoupled nonlinear equations. This was done because the subroutine NS01A will solve for a minimum of two equations. The inputs are stated in the program. Again, dimensioning is very important. Arrays which are dimensioned in the main program should be dimensioned the same in subroutine(s) that they are used in.

Those arrays or variables which are declared real, integer, complex, etc. must be declared the same in the subroutine(s) that they are used in. In the subroutine PLOTT, the routine AROHD is an auxiliary routine of the ASD Calcomp Plot routines. AROHD is available on a library called CCAUX and must be attached in the control cards.

VITA

Paul L. Vergez was born in New Orleans, Louisiana in January 1955. He graduated from the University of New Orleans in May 1977 and was awarded the degree of Bachelor of Science in Electrical Engineering. He was commissioned a 2nd Lt through AFROTC. His initial Air Force assignment was to report to AFIT, Wright-Patterson AFB, Ohio, in September 1977. His assignment after graduating from AFIT is to report to the Air Force Weapons Laboratory, Eglin AFB, Florida.

Permanent Address: 76 Mason Avenue  
Gretna, Louisiana 70053

UNCLASSIFIED

SECURITY CLASSIFICATION OF THIS PAGE (When Data Entered)

REPORT DOCUMENTATION PAGE		READ INSTRUCTIONS BEFORE COMPLETING FORM
1. REPORT NUMBER AFIT/GGC/EE/79-4	2. GOVT ACCESSION NO.	3. RECIPIENT'S CATALOG NUMBER
4. TITLE (and Subtitle) INVESTIGATION OF ROLL PERFORMANCE FOR A HIGHLY NONLINEAR STATICALLY UNSTABLE FIGHTER-TYPE AIRCRAFT		5. TYPE OF REPORT & PERIOD COVERED MS THESIS
		6. PERFORMING ORG. REPORT NUMBER
7. AUTHOR(s) Paul L. Vergez 2 Lt. USAF		8. CONTRACT OR GRANT NUMBER(s)
9. PERFORMING ORGANIZATION NAME AND ADDRESS Air Force Institute of Technology (AFIT/EN) Wright-Patterson AFB, Ohio 45433		10. PROGRAM ELEMENT, PROJECT, TASK AREA & WORK UNIT NUMBERS
11. CONTROLLING OFFICE NAME AND ADDRESS AFFDL/FGC Wright-Patterson AFB, OH 45433		12. REPORT DATE March 1979
		13. NUMBER OF PAGES 85
14. MONITORING AGENCY NAME & ADDRESS (if different from Controlling Office)		15. SECURITY CLASS. (of this report) UNCLASSIFIED
		15a. DECLASSIFICATION/DOWNGRADING SCHEDULE
16. DISTRIBUTION STATEMENT (of this Report)  APPROVED FOR PUBLIC RELEASE: DISTRIBUTION UNLIMITED		
17. DISTRIBUTION STATEMENT (of the abstract entered in Block 20, if different from Report)		
18. SUPPLEMENTARY NOTES APPROVED FOR PUBLIC RELEASE; IAW AFR 190-17  JOSEPH P. HIPPS, Major, USAF 16 MAY 1979 DIRECTOR OF INFORMATION		
19. KEY WORDS (Continue on reverse side if necessary and identify by block number) Stability Roll Performance Bifurcation Analysis Catastrophe Theory		
20. ABSTRACT (Continue on reverse side if necessary and identify by block number) A linearized model of a fighter-type aircraft with significant roll-pitch inertial coupling, including its full flight control system is required in order to conduct a comparative analysis between body axis rolls and velocity (stability) axis rolls. The stability of the aircraft is checked at various roll rates for both body axis and velocity axis rolls. This is done by examining the signs of the eigenvalues of the linearized model-positive for unstable		

DD FORM 1 JAN 73 1473

EDITION OF 1 NOV 65 IS OBSOLETE

UNCLASSIFIED

SECURITY CLASSIFICATION OF THIS PAGE (When Data Entered)

and negative for stable. It is found that at various angles of attack the velocity axis rolls prove to be at least as stable and, in most cases, more stable than body axis rolls. The stability is also observable for various combinations of flight control systems.

In developing a nonlinear coupled equation solver, a single equation with known solutions is considered first. This is done to show a simplified version of what the nonlinear program is required to do. Next, a pair of nonlinear coupled equations is analyzed. The development of the program for the single equation case proves to be successful, but certain problems arise when working with a pair of coupled equations. This thesis provides a good foothold on a method of analysis known as Bifurcation Analysis and Catastrophe Theory which can be used to solve the nonlinear coupled aircraft equations. This thesis presents some of the problems which could be encountered.